1-1-2011

Catalytic activity of titania and titania-containing nanomaterials: And, Spatial distribution of silica surface groups using a tethered amine catalyst

Ramkumar Samala
Eastern Illinois University

This research is a product of the graduate program in Chemistry at Eastern Illinois University. Find out more about the program.

THESIS MAINTENANCE AND REPRODUCTION CERTIFICATE
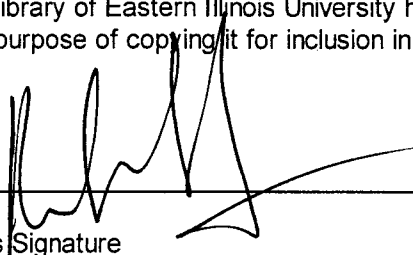
TO: Graduate Degree Candidates (who have written formal theses)

SUBJECT: Permission to Reproduce Theses

The University Library is receiving a number of request from other institutions asking permission to reproduce dissertations for inclusion in their library holdings. Although no copyright laws are involved, we feel that professional courtesy demands that permission be obtained from the author before we allow these to be copied.

PLEASE SIGN ONE OF THE FOLLOWING STATEMENTS:

Booth Library of Eastern Illinois University has my permission to lend my thesis to a reputable college or university for the purpose of copying it for inclusion in that institution's library or research holdings.

_____   09 / 20 / 2011 _____

Author's Signature   Date

I respectfully request Booth Library of Eastern Illinois University **NOT** allow my thesis to be reproduced because:

_____

_____

_____

_____   _____

Author's Signature   Date

This form must be submitted in duplicate.

Catalytic Activity of Titania and Titania Containing Nano Materials;

Spatial Distribution of Silica Surface Groups Using a Tethered Amine Catalyst

(TITLE)

BY

Ramkumar Samala

THESIS

SUBMITTED IN PARTIAL FULFILLMENT OF THE REQUIREMENTS
FOR THE DEGREE OF

Masters of Science in Chemistry

IN THE GRADUATE SCHOOL, EASTERN ILLINOIS UNIVERSITY
CHARLESTON, ILLINOIS

2011

YEAR

I HEREBY RECOMMEND THAT THIS THESIS BE ACCEPTED AS FULFILLING
THIS PART OF THE GRADUATE DEGREE CITED ABOVE

THESIS COMMITTEE CHAIR   DATE

DEPARTMENT/SCHOOL CHAIR   DATE
OR CHAIR'S DESIGNEE

THESIS COMMITTEE MEMBER   DATE

THESIS COMMITTEE MEMBER   DATE

THESIS COMMITTEE MEMBER   DATE

THESIS COMMITTEE MEMBER   DATE

Catalytic activity of titania and titania-containing nanomaterials and Spatial distribution of silica surface groups using a tethered amine catalyst

By

Ramkumar Samala

ABSTRACT

Titania and titania-containing nanomaterials are semiconductor photocatalysts and are widely used to degrade (i.e. oxidize) organic matter. The adsorption and catalytic properties of highly dispersed titania prepared using sulfate and pyrogenic methods, and fumed containing mixed oxides, were studied using catalytic decomposition of methylene blue primarily by kinetic methods. Commercial ultrafine titania (PC-100, PC-105 and PC-500), fumed TiO_2, and the mixed oxide of 80% Silica/20% Titania (ST20) were studied. Catalytic activity as measured by methylene blue decomposition kinetics was highest per gram for non-treated ultrafine titania PC-500 which has the highest S_{BET} and smallest particle size. However this activity per m^2 was higher for PC-105, having a smaller S_{BET} value than PC-500. When it comes to activity per unit surface area of titania ST20 had the highest catalytic activity.

Heating of the titania affects the catalytic activity which was observed on PC-500. PC-500 heated at 650°C had higher catalytic activity than the titania heated at 800°C and 900 °C. This is due to the enhancement of anatase content at 650°C and rutile content at 800°C and 900 °C.

Aminosilanes are the most widely used organosilanes because of their wide range of applications and their use as precursors for the modification of silica surfaces. The choice of aminosilane and silica is essential for controlling their amount, stability and distribution on the surface of the silica. Comparison of trialkoxy silanes between APTES and ABTES clearly indicate that increase in chain length in ABTES increases the catalyzing action in silica gels exception in pyrogenic silica. Aminosilanes with the same chain length but different number of hydrolysable groups show monoalkoxysilane APDMES having more flexibility than trialkoxysilanes APTES and ABTES to catalyze TMMS. When the number of amine groups

increases in the aminosilane the chances of forming clumps or restricted movement increases as seen in AEIDMS in catalyzing TMMS.

Comparison among the silicas clearly indicates HS-5 composed of solid non-porous primary particles of approximately 10nm was able to catalyze higher TMMS. Among the silica gels, 200DF given its narrow pore nature and cross-linking had least catalyzation of TMMS for trialkoxy silanes.

Acknowledgment

I would like to express my sincere thanks to Dr. Jonathan Blitz for giving me an opportunity to pursue research under his guidance and for his support, encouragement and patience throughout this project.

My thanks and appreciation goes to my thesis committee members, Dr. Barbara Lawrence, Dr. Svetlana Mitrovski and Dr. Douglas Klarup.

I would like to extend my sincere thanks to Dr.Svetlana Mitrovski for helping to analyze the samples and also guiding in the absence of my advisor.

Last but not least, I thank all of my friends and family. Each of you can share in this accomplishment, for without your support it would not have been possible. I would also thank Eastern Illinois University for giving me an opportunity to study in here.

TABLE OF CONTENTS

LIST OF TABLES

LIST of Figures

Chapter 1: Catalysis of titania and titania containing nanomaterials.

Chapter 2: Amine catalysis of organosilyation reactions with tethered silane to probe the spatial distribution of reactive silica surface groups

Chapter 1

Catalytic activity of titania and titania-containing nanomaterials

1.1 Introduction

The treatment of ground water contamination by industrial waste is one of the important studies going on around the world[2]. Various traditional methods such as biological oxidation, chemical oxidation, and adsorption[3, 4] have been used but have generally recognized drawbacks. Biological oxidation is restricted by operating costs, pH, temperature control, etc. Chemical oxidation may not result in complete oxidation, and adsorption does not result in the elimination of contaminants, adsorbents merely transfer the contaminants from the liquid to the solid phase adsorbent. Photodegradation by semiconductor catalysts is an alternate method for the treatment of groundwater contamination with some realized and potential advantages[5]. The advantages include complete dissociation of organic matter into CO_2 and H_2O, easy separation from reactants, economical, reactions occur at room temperature, etc[6].

Semiconductor photocatalysts (e.g., TiO_2, ZnO, Fe_2O_3, CdS, and ZnS) are light sensitizers which catalyze light-reduced redox processes because of their characterized filled valence band and an empty conduction band[7]. When a photon from a light source hits a semiconductor particle like TiO_2 that matches or exceeds the energy of the band gap, an electron jumps from the valence band to the conduction band, leaving a hole in the valence band. These excited conduction-band electrons and valence band holes can recombine and dissipate energy or react with electron donors and acceptors on the surface of the catalyst. The valence holes are powerful oxidants and can react with organic compounds to oxidize them[8], whereas the conduction electrons are good reductants.

13
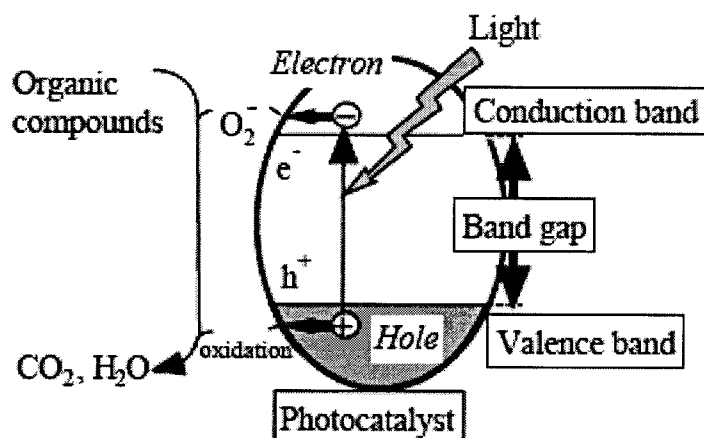
Figure 1.1 Mechanism of photocatalyis   (Downloaded from

http://www.mechnanosolutions.com/mechanism.html)

Mechanism of Oxidation

Photoexcitation: $TiO_2 + hv$ (photon) $\longrightarrow$ e^- (electron) $+ h^+$ (hole)

$$H_2O + h^+ \longrightarrow OH^{\bullet} + H^+$$
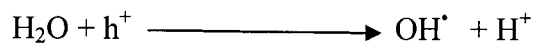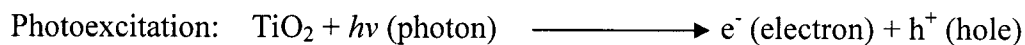
The $^{\bullet}OH$ radicals initiate the oxidation of organic compounds to carbon dioxide and water[9, 10]:

Let us see an example of photooxidation of formaldehyde[11]:

$$HCHO + {}^{\bullet}OH \longrightarrow CHO^{\bullet} + H_2O$$

$$CHO^{\bullet} + OH \longrightarrow HCOOH$$

$$HCOOH + {}^{\bullet}O_2 \longrightarrow HCO_3^- + H^+$$

$$HCO_3^- + H^+ \longrightarrow HCOOOH$$

$$HCOOOH + HCHO \longrightarrow 2HCOOH$$

14

$$\text{HCOOH} \xrightarrow{\text{-H}} \text{HCOO}^{\bullet} \xrightarrow{\text{OH}} \text{H}_2\text{O} + {}^{\bullet}\text{CO}_2$$

$$\text{HCOO}^{\bullet} \xrightarrow{\text{h}^+} \text{H}^+ + {}^{\bullet}\text{CO}_2$$

$${}^{\bullet}\text{CO}_2 \xrightarrow{\text{OH,h}^+,(\text{O})} \text{CO}_2$$
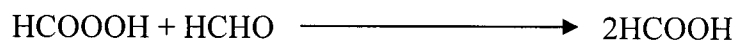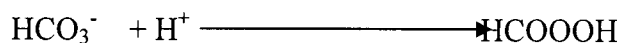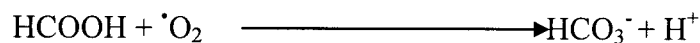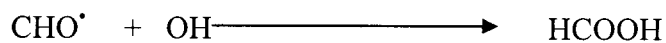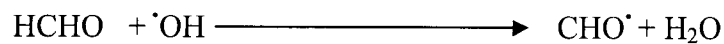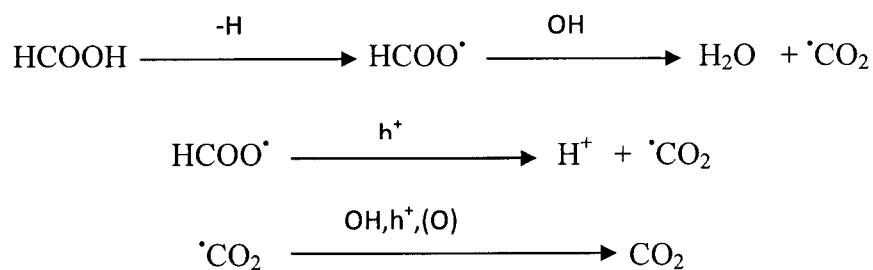
Among semiconductor photocatalysts, titania (TiO_2) has been widely used. Such uses have included the destruction of microorganisms[12-16] and the oxidation of organic matter at ambient temperature and pressure. Titania is also non-toxic and inexpensive. Titania is a white pigment and occurs predominantly in two crystalline forms, anatase and rutile. Anatase is photocatalytically more reactive than the rutile form and absorbs radiation below 384 nm in the UV region of the spectrum. Many variables affect photocatalytic property of these titania such as surface area[17], surface adsorption properties[18, 19], presence of surface functionalities[20-22], ratio of anatase to rutile[23-25] etc. Fumed titania is prepared by hydrolysis of $TiCl_4$ at high temperatures in oxygen-hydrogen flame. On the other hand, highly pure TiO_2 nanomaterials and mixed oxides of SiO_2/ TiO2 are synthesized pyrogenically in a H_2/N_2O_2 flame[26-31]. These fumed titania showed different phase composition of anatase and rutile form which is an important characteristic for industrial applications.

Silica is an oxide of metal silicon, in which the silicon atom is tetrahedrally coordinated with 4 oxygen atoms (SiO_4) to form a building block of silica (SiO_2). Fumed silicas or pyrogenic silica are made by flame pyrolysis of silicon tetrachloride or quartz at 3000°C. The fumed mixtures of SiO_2/TiO_2 are mixed at the chemical level, not at a physical level to enhance the stability and catalytic activity of titania.

Various properties affect the catalytic behavior of titania such as phase composition, pore structure, pore size, and particle size. These surface and textural properties of titania greatly depend on the method of preparation. In these studies titania synthesized pyrogenically from H_2/N_2O_2 flame, liquid phase synthesis by sulfate method, and fumed titania containing mixed oxides are compared. Residual sulfate plays an important role in photocatalysis as shown by studies reported on temperature dependent phase behavior, enhancement of particle flocculation and diminution of the band gap (E_g). Understanding the structure/catalytic activity relationships of these titania materials can aid in the improvement of these materials.

. In order to understand these effects, different titania synthesized from various methods are compared by studying the catalytic decomposition of methylene blue. Methylene blue is a water soluble textile dye widely used in the TiO_2 decomposition studies in aqueous solutions. Methylene blue is an industrial dye and gives a blue color when dissolved in water. It has been widely used in titania photodecomposition studies in aqueous solutions to determine the catalytic activity of various forms of titania. It is also used as a staining agent in biological applications. It has a molecular formulae $C_{16}H_{18}N_3SCl$ and the structure is shown in Fig 1.2. Methylene blue solution is a redox indicator which is blue color in oxidized form and turns colorless in the presence of reducing agent.
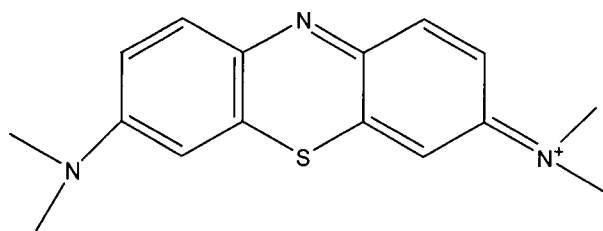
Figure 1.2 Structure of methylene blue

The convenience of using dyes to test degradation kinetics is that visible spectrophotometry can be readily utilized. UV-vis spectroscopy is the most widely used analytical technique for quantitative determination of analyte concentration. It is used to measure the concentration of methylene blue in the adsorption and photocatalytic experiments in this work. Methylene blue is a conjugated chromophore which absorbs visible light at certain wavelengths According to the Beer-Lambert law absorbance is directly proportional to the concentration and path length at a constant wavelength. By knowing the absorbance at λ_{max} for different methylene blue solutions the concentration can be calculated by the equation below.

According to the Beer-Lambert law

$$A = \varepsilon c l$$

Where: ε - Molar absorptivity coefficient (Mcm^{-1})

l - path length (cm)

c - Concentration of the analyte (M or mol/dm^3)

1.1.1 Kinetics

Since the ability of the semiconductor catalysts to decompose methylene blue will be evaluated by a kinetics analysis, a brief description of these kinetics follows.

A rate of a reaction is defined as the change in concentration of reactants or products per unit time. For example,

$$aA + bB \rightarrow cC$$
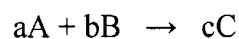
$$Rate = k\,[A]^m\,[B]^n$$

where k is the rate constant, A and B are concentration of reactants and m and n are the reaction order with respect to A and B. The reaction rate at any point in a concentration *vs* time graph is found by measuring the slope of the graph as a tangent (1st derivative) at that point. The steeper the slope, the faster the rate of the reaction.

In order for a reaction to occur at the surface of a solid particle in a heterogeneous system, the reactant(s) must first diffuse to the catalytically active site. If such a reaction is diffusion rate limited, then for a 1 reactant system the reaction will follow first order kinetics. In this case for the reactant A (methylene blue), the rate is given by the following relation:

$$Rate = \frac{d(A)}{dt} = k\,[A]dt$$

Where: k -First order rate constant and [A] -Concentration of reactant A

$$\frac{dA}{dt} = -kt$$

$$dA = -k[A]dt$$

$$\frac{dA}{[A]} = -k\,dt$$

$$\int_{A0}^{At} \frac{dA}{[A]} = -k \int_{0}^{t} dt$$

$$\ln[A]_{A0}^{At} = -k[t]_{0}^{t}$$

18

$$\ln\left[\frac{At}{A0}\right] = -kt$$

$$\ln[A]_t = -kt + \ln[A]_0$$

Which is in the form of $y = mx + b$

Where A_t- concentration of A at time t=t and A_0-concentration of A at time t=0(initial concentration) and k, the rate constant is the slope.

A reaction is first order if the plot $\ln[A]_t$ *vs* t gives a straight line, which should be the case for the diffusion rate limited decomposition of methylene blue.

1.2 Materials and Methods

1.2.1 Materials

1.2.1.1 Methylene Blue: Methylene blue (3, 7-bis (Dimethylamino)-phenothiazin-5-ium chloride), CAS number 18015-76-4 was purchased from National Aniline and Chemical Co Inc. NY, USA. Distilled Millipore® water was used to prepare different concentrations of Methylene blue solution.

1.2.1.1 Catalysts: Commercial ultrafine Titania (PC-100, PC-105 and PC-500) were received from Millenium Inorganic Chemicals, Research Center, Baltimore, MD, USA. Other titania nanomaterials (fumed TiO_2, (ST20) Silica/titania) were received from the Institute of Surface Chemistry, Kalyush, Ukraine. The characteristics of these catalysts are listed in table 1.1.

Table 1.1 Characteristics of catalysts

Sample	Specific surface area S_{BET} (m^2/g)
PC-100	89
PC-105	78
PC-500	207
Fumed TiO_2	60
ST20	64

A more detailed analysis of these materials can be found in reference 1.

1.2.2 Instrumentation

1.2.2.1 Light source: A 275 Watt UV lamp (General Electric) with emission lines at 312 nm and 365 nm was used as the photocatalytic light source.

1.2.2.2 UV spectroscopy: A Shimadzu UV3100 spectrometer was used to record the absorbance of various concentrations of methylene blue. The absorbances were recorded at 660 nm using a 1-cm glass cuvette.

1.2.3 Methods

1.2.3.1 Photochemical decomposition of Methylene Blue by various catalysts

A 500 ppm stock solution of Methylene blue was prepared by adding 0.2503 g of Methylene blue to 500 mL of Millipore water in a volumetric flask. Fresh stock solutions of 20 ppm were prepared for every experiment by dilution. A volume of 200 mL of (20 ppm) methylene blue solution was taken in a 500 mL flask and the pH was adjusted to 7.0 by the addition of dilute NaOH, after which the absorbance was recorded. To the solution 0.2 g of catalyst was added and the slurry was stirred for 20 minutes in the dark and the absorbance of the solution was recorded. The slurry was than irradiated with UV light with constant stirring to avoid settling and constant exposure of the catalyst. Samples were collected at regular intervals for a time period of 45 minutes and their absorbances were recorded.

1.3 Results and Discussion

1.3.1 Photochemical decomposition of methylene blue in the presence of various catalysts

In this section the catalytic behavior of various catalysts and their kinetics are compared based on the decomposition kinetics of methylene blue and their rate constants.

The maximum absorption wavelength (λ_{max}) of methylene blue was 660 nm as shown by the absorption spectrum of Figure 1.3. The λ_{max} was used as a calibration point for the determination of all the absorbance measurements in this work. A calibration line was plotted for different concentrations with the methylene blue versus absorbance in Figure 1.4. This shows that absorbance values followed the Beer-Lambert law which was determined by the linearity of the plot. Fresh stock solutions of 20 ppm were prepared for every experiment by dilution and a weighed amount of catalyst was added to the solution. After the addition the mixture was kept in the dark for 20 minutes for the absorption to reach equilibrium between the catalyst and the dye. At this point the sample collected was recorded as initial reading. After this the reaction mixture was irradiated with the UV light and the samples are collected at regular time intervals. The samples were centrifuged to separate methylene blue solution from adsorbents and diluted by a suitable dilution factor such that the absorbance was within the calibration range and the absorbances were collected by UV-vis spectroscopy.

Plots of photocatalytic decomposition reactions of various catalysts i.e.; concentration of methylene blue remaining in the solution versus the irradiation time of UV light are shown in Figures 1.5-1.9. Rate constants are calculated from the slope by plotting ln C vs time as shown in Figures 1.10-1.14 to determine the kinetics of the reaction. From the rate constants normalized to

surface area shown in Table 1.3, the methylene blue rate constants decrease in the order PC-105 >_PC-100_>_ fumed TiO_2 _>_PC-500 and ST20. The reaction rate is determined by drawing a tangent line to the slope at any point of the curve which determines the rate at that particular point. Rate constant is the proportionality constant that expresses the relationship between the rate of a chemical reaction and the concentrations of the reactants and products. Analysis of the rate reaction plots from Figures 1.5-1.9 show that the photodecomposition of methylene blue roughly follows first order kinetics by the nearly linear plots of ln C vs time in Figures 1.10-1.14 except for PC-105 which follow zero order kinetics. The difference in the rate constant is mainly attributed to the method of preparation and their structural characteristic of titania by which the photocatalytic activity is affected.

1.3.2 Comparison of Photocatalytic decomposition of ultrafine titania and fumed TiO_2

From Figure 15 and Table 1.2 comparison among the commercial ultrafine titania (PC-100, PC-105 and PC-500) and fumed TiO_2, the degradation rates and rate constants clearly indicate that PC-500 is the superior catalyst for methylene blue degradation. PC-500 has a relatively large surface area and few sulfate functionalities, as it was manufactured from sulfate free reactants, both potentially beneficial to this catalyst's activity. Sulfate groups on titania have various effects on catalytic activity such as increasing the coagulation of particles due to the decrease in EDL (electrical double layer) layer and increase in ionic strength by decreasing repulsion between particles[20-22]. The titania prepared from the sulfate process, PC-100 and PC-105, are prone to coagulation perhaps resulting in less photocatalytic activity than PC-500. Sulfur containing titania have other advantages such as their ability to withstand the conversion of anatase to rutile formation and the ability to withstand sintering at high temperatures which

can be seen in reference 1. This effect is because loss of sulfur is endothermic and the anatase to rutile transition is exothermic, so a higher activation energy (temperature) is required for sulfur contaning titania for the phase conversion. Although when catalyst activity normalized to total surface area by the formulae $A = \frac{C_{MB,o} - C_{MB}}{C_{MB,o}} / S_{BET}$, Figure 1.16 and table 1.3 clearly shows that PC-105, having a smaller S_{BET} than PC-500, showed higher catalytic activity per m^2.

From Figure 1.15 it is clear that fumed TiO$_2$ has the lowest catalytic activity among all other titania which may be due to several reasons such as its lower S_{BET} and its reduced hydrophilicity.The reduced hydrophilicity occurs at high temperature due to the condensation of surface hydroxyl groups. Reduction in hydroxyl groups usually affects the catalytic activity by decreasing the binding affinity and by increasing the coagulation among the particles. Fumed titania are manufactured at high temperatures which may result in titania crystallizing in the catalytically less active rutile form when compared to other catalysts.

1.3.3 Comparison of ST20 with other catalysts

Comparison of decomposition plots between ST20 and other catalysts showed different trends. For example, Figure 1.17 shows that ST20 adsorbs much more methylene blue than all other catalysts. Methylene blue is a cationic dye and it adsorbs strongly towards ST20, a more hydrophilic catalyst than all other catalysts. The presence of hydroxyl groups originating from silica from the mixed oxide makes it more hydrophilic and makes it adsorb more methylene blue. Although it has the least catalytic activity as measured per gram among all the titania, considering only the content of this material is only 20% titania it has the most active titania phase. In other words the photocatalytic activity normalized to titania content from the Figure 1.18 is highest compared to all other photocatalytic materials.

24

1.3.4 Comparison of PC-500 heated to different temperatures

In this set of experiments PC-500 was heated to 3 different temperatures; 650°C, 800°C and 900°C. Figure 1.19 shows the comparison of catalytic activity of unheated PC-500 and PC-500 heated to different temperatures. From this data it can be clearly seen that PC-500 heated to 650°C has the highest methylene blue photodecomposition rate. Heating of titania strongly affects the catalytic activity as the titania transforms from the more photocatalytical active phase anatase to the less active phase of rutile. It also effects phase transformation by converting titania from amorphous to crystalline form. Both of these temperature effects can be seen from powder x-ray diffraction data detailed in reference 1. The factors contributing to greater catalytic activity at a treatment temperature of 650°C are at least 2-fold: at this temperature the anatase → rutile transformation has not yet occurred; and the transformation of amorphous to crystalline titania which has. These conclusions are reached from xrd analysis detailed in reference 1.
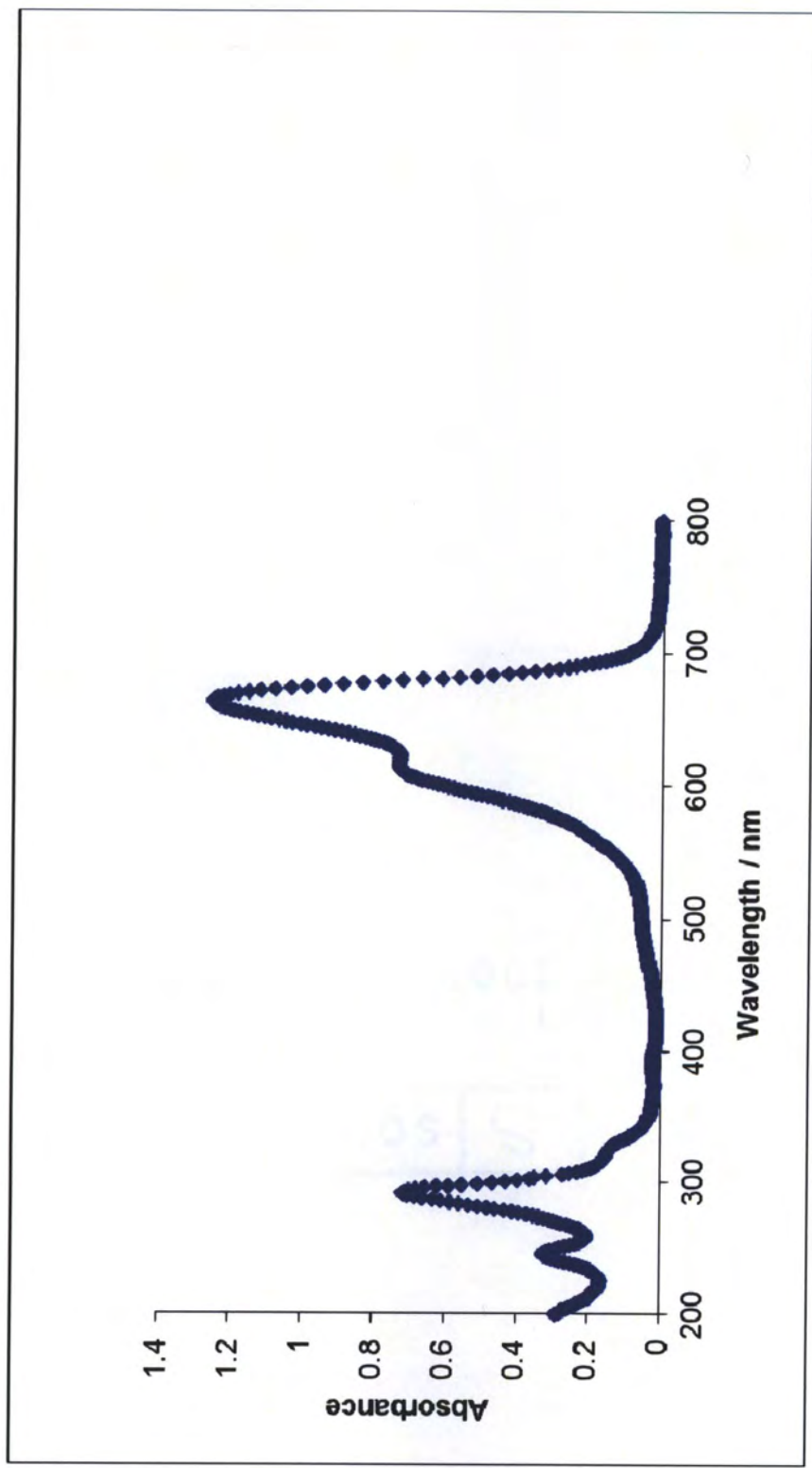
Figure 1.3 Absorption spectrum of methylene blue.
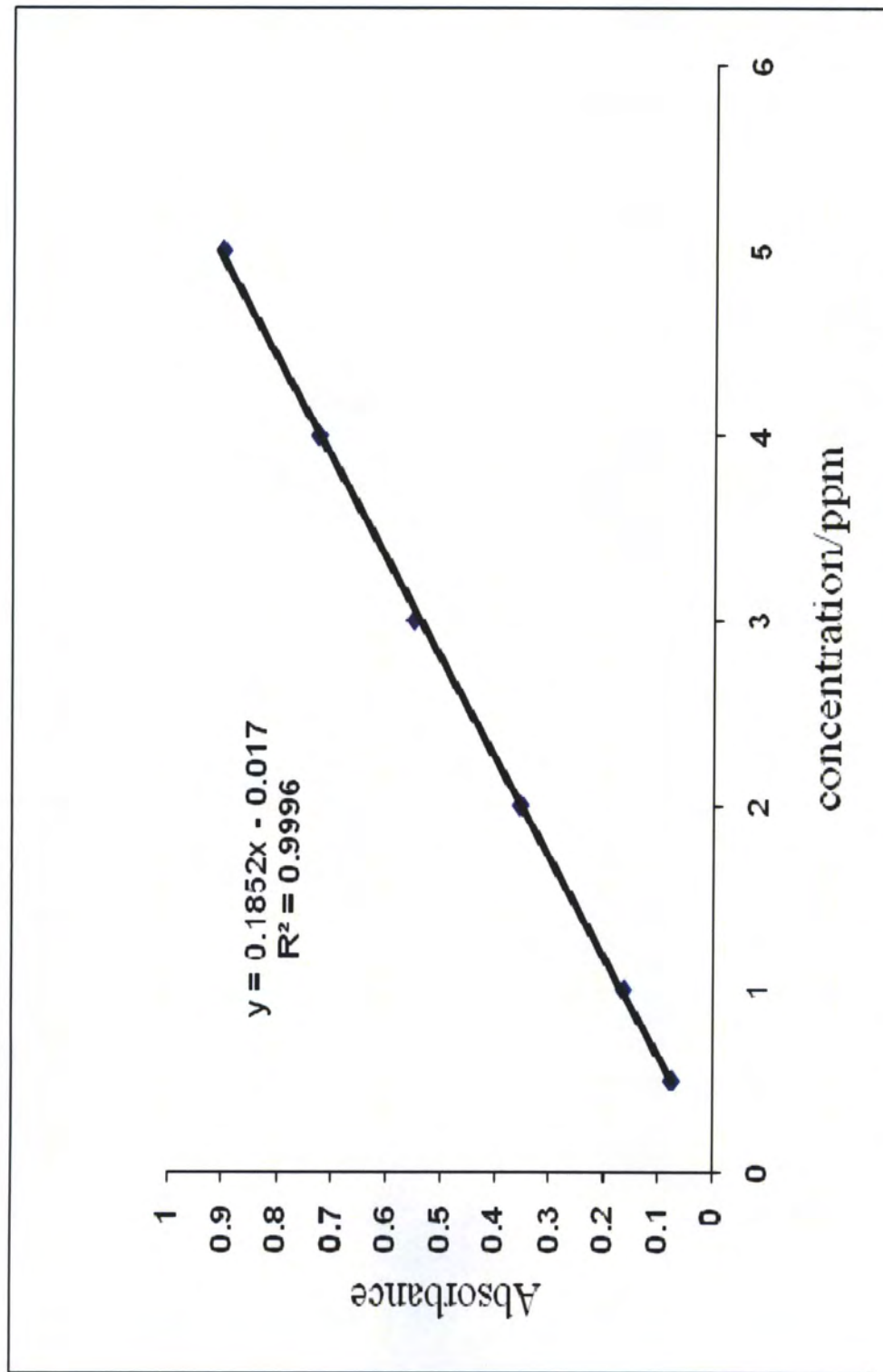
Figure 1.4 Calibration curve of methylene blue absorbance recorded at 660 nm.

y = 0.1852x - 0.017
R^2 = 0.9996

concentration/ppm

Absorbance
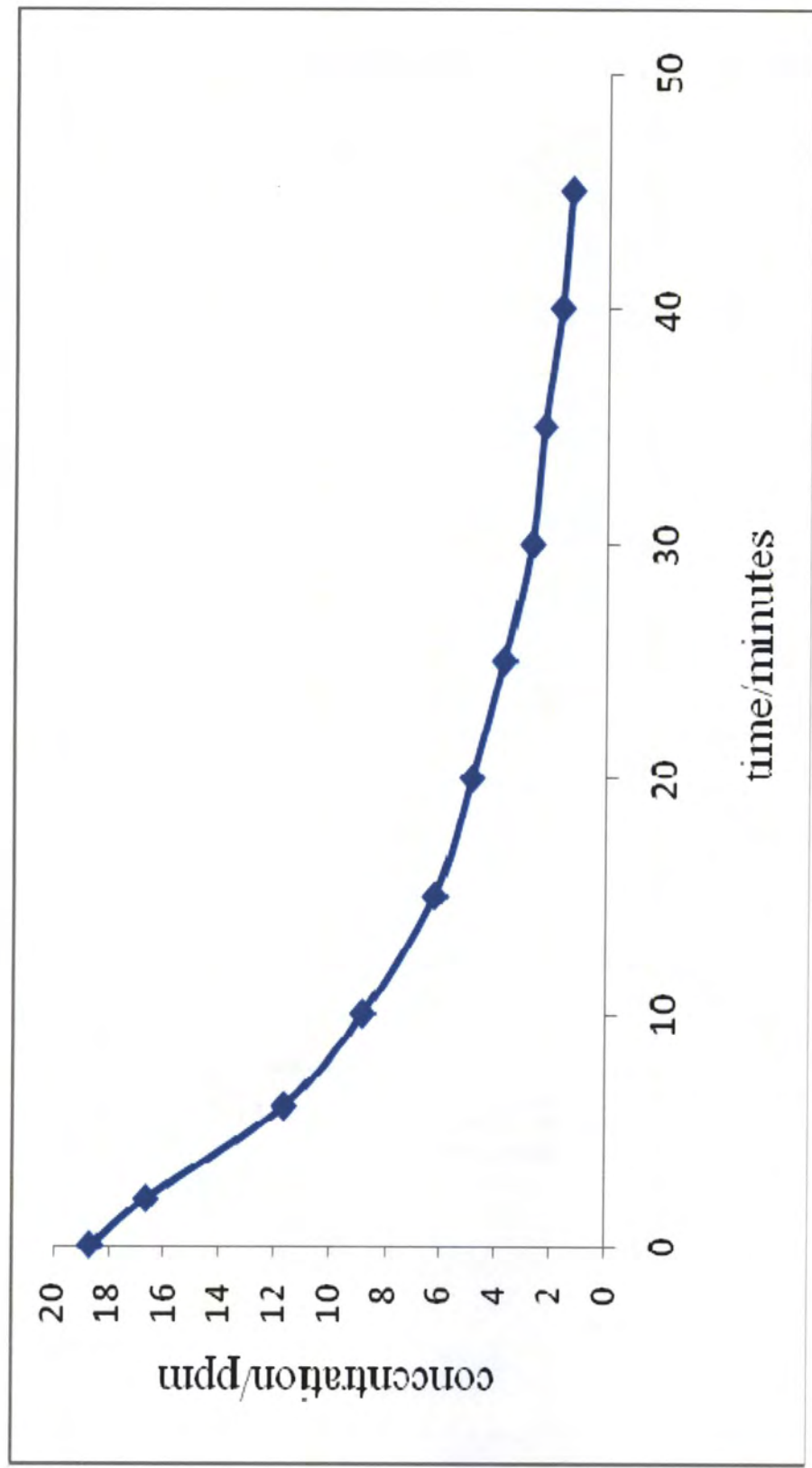
Figure 1.5 Decomposition curve for methylene blue in the presence of UV irradiation as a function of time with PC-500 catalyst.
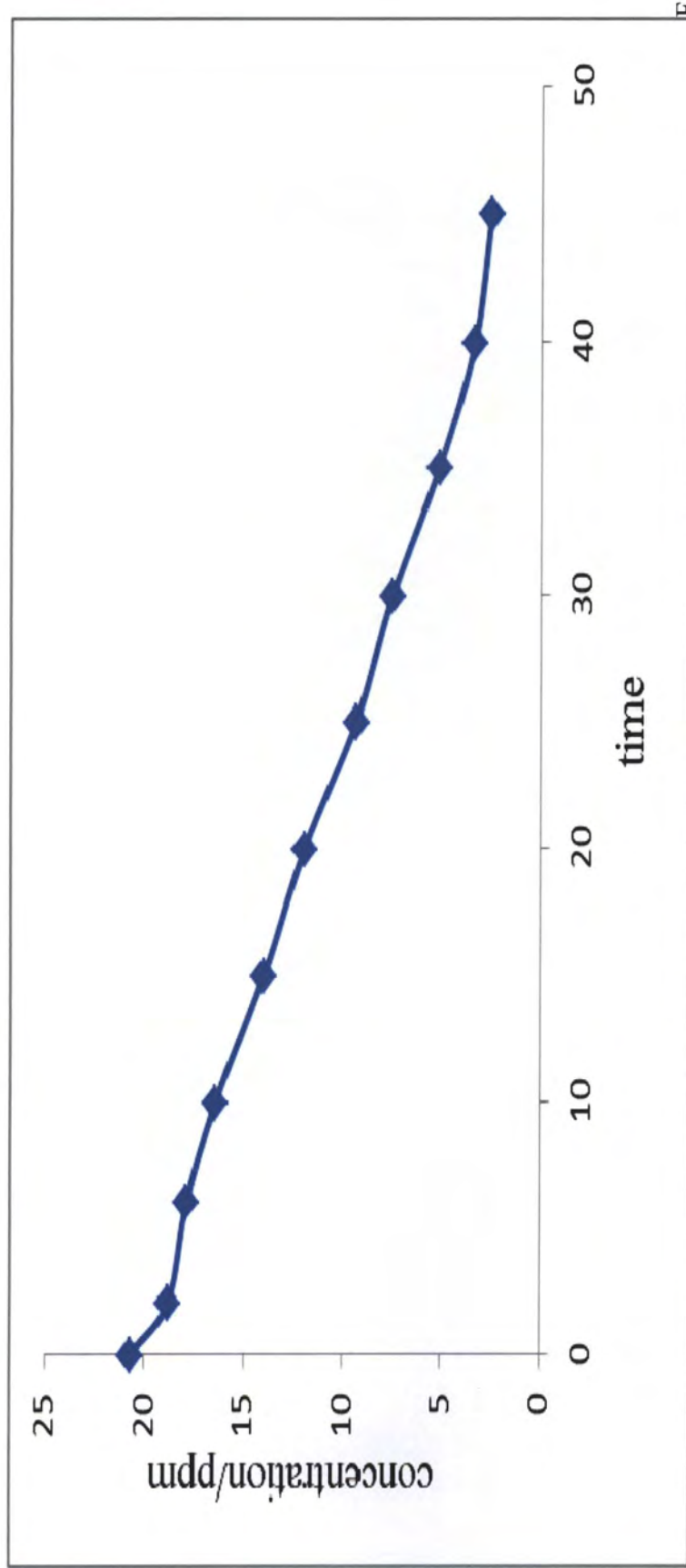
Figure 1.6 Decomposition curve for methylene blue in the presence of UV irradiation as a function of time with PC-105 catalyst.

29
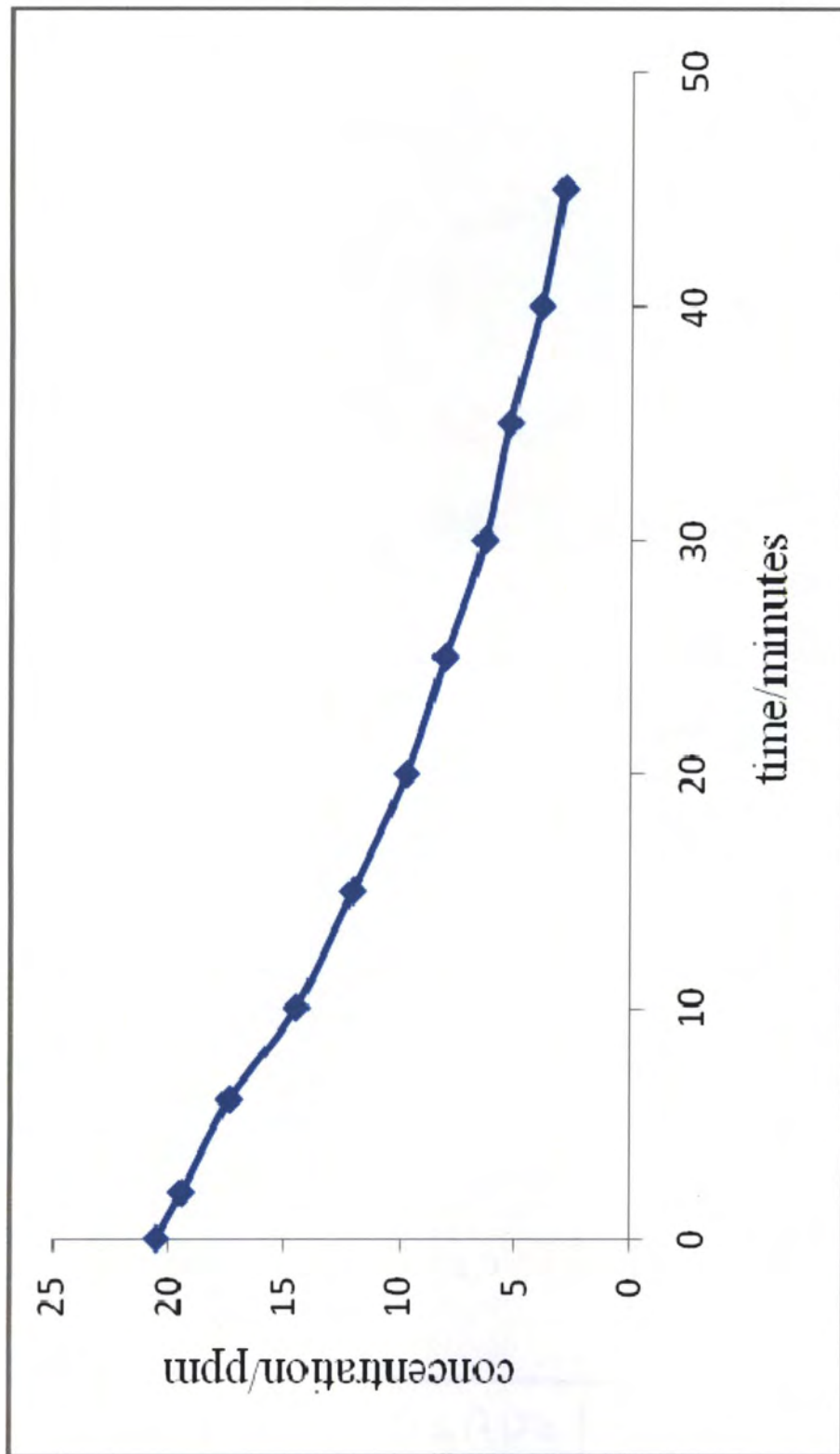
Figure 1.7 Decomposition curve for methylene blue in the presence of UV irradiation as a function of time with PC-100 catalyst.
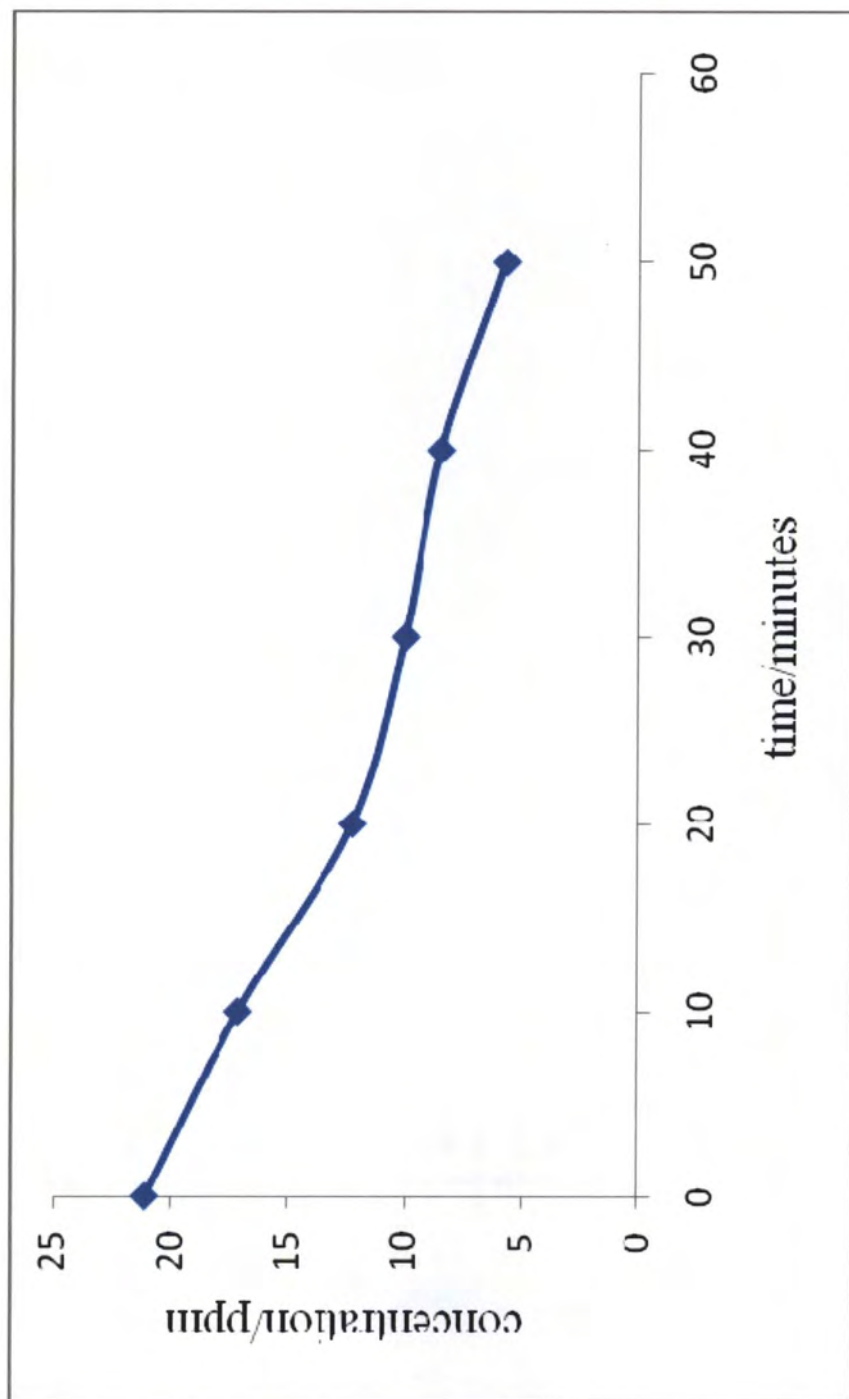
Figure 1.8 Decomposition curve for methylene blue in the presence of UV irradiation as a function of time with fumed TiO_2 catalyst.
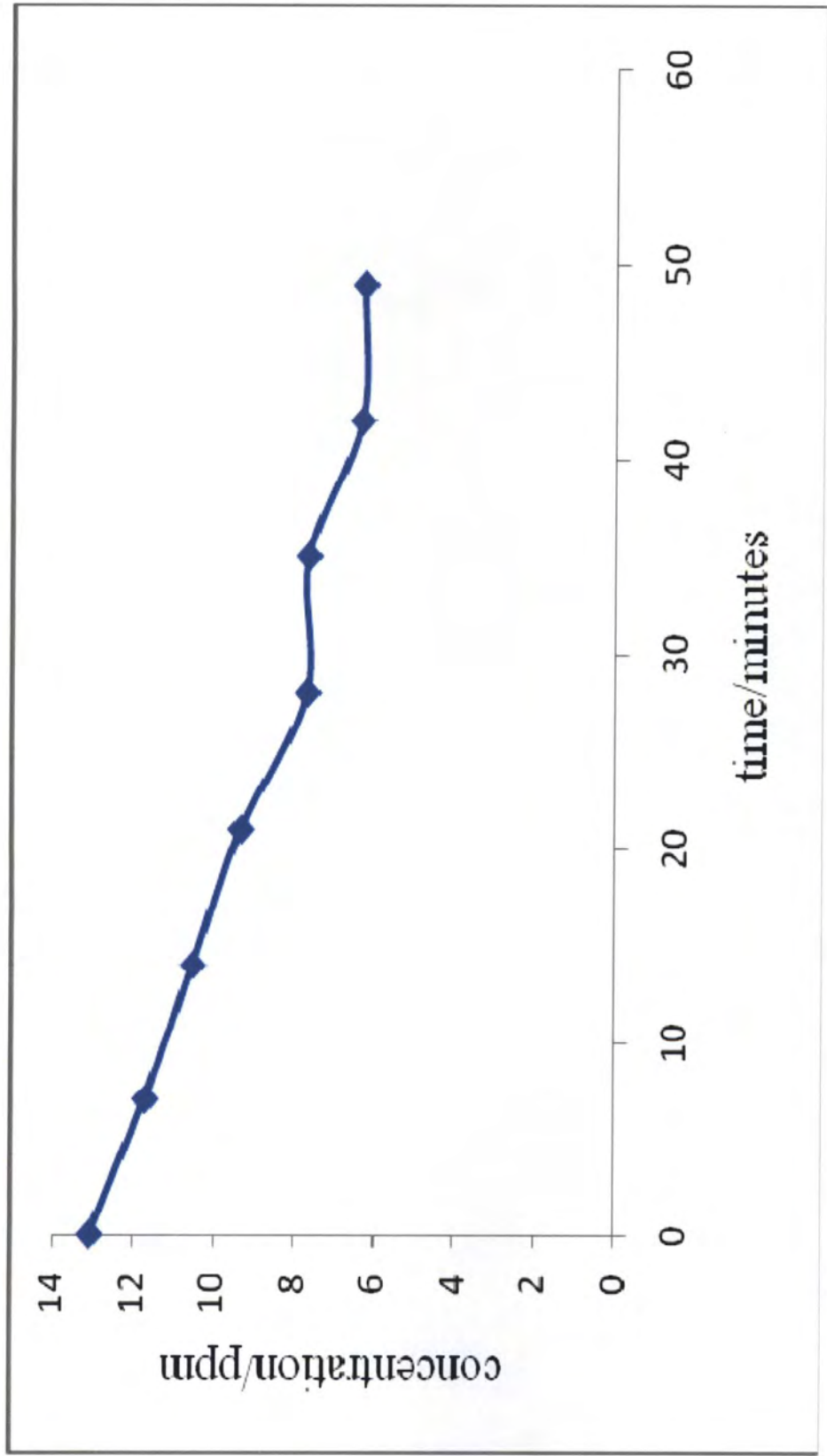
Figure 1.9 Decomposition curve for methylene blue in the presence of UV irradiation as a function of time with ST20 catalyst.
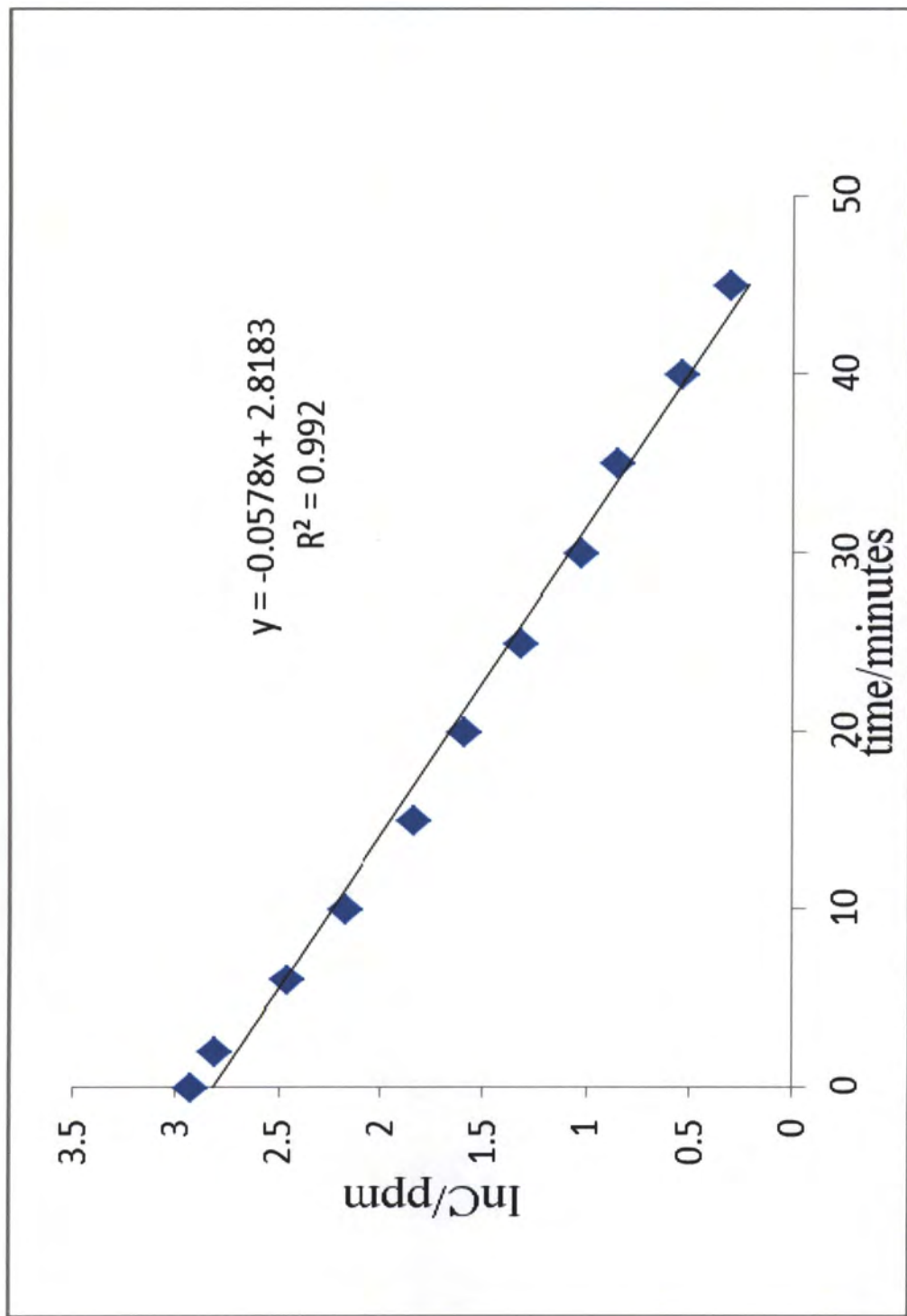
Figure 1.10 First order kinetics plot of the PC-500 mediated methylene blue decomposition. Data taken from Figure 5.

The chart shows a plot of $\ln C$/ppm versus time/minutes with the fitted line:

$$y = -0.0578x + 2.8183$$
$$R^2 = 0.992$$
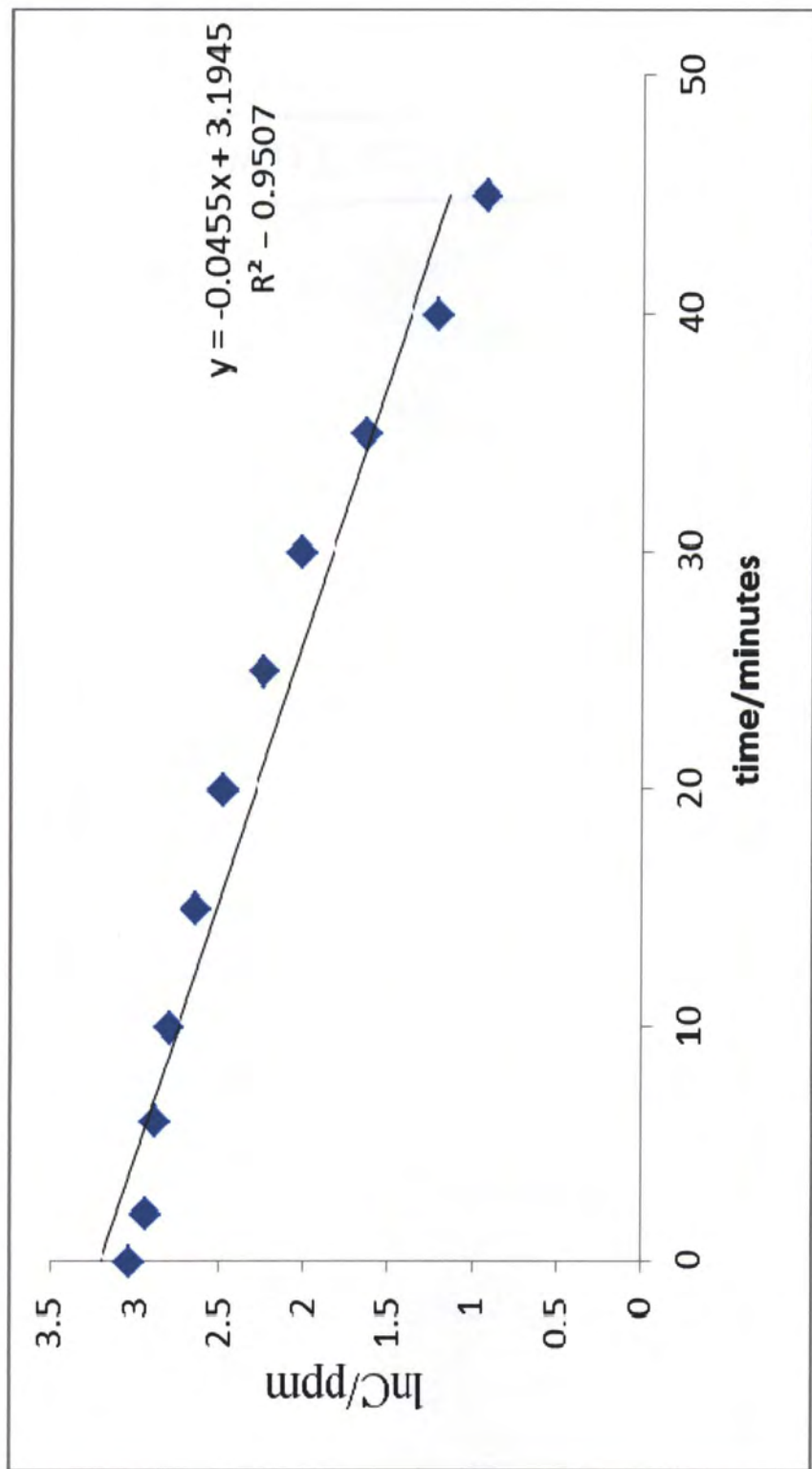
Figure 1.11 Zero order kinetics plot of the PC-105 mediated methylene blue decomposition. Data taken from Figure 6.

34
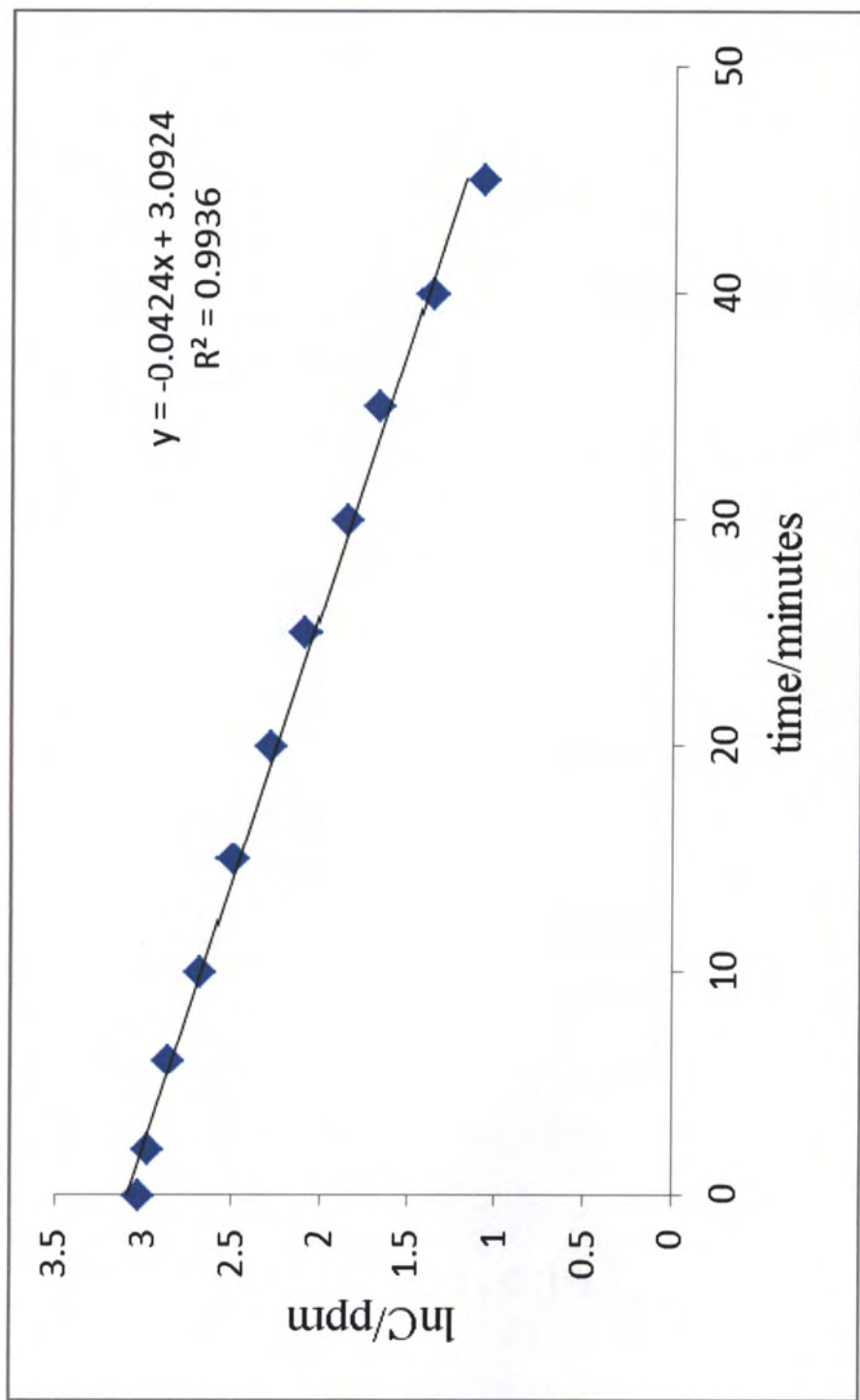
Figure 1.12 First order kinetics plot of the PC-100 mediated methylene blue decomposition. Data taken from Figure 7.

35
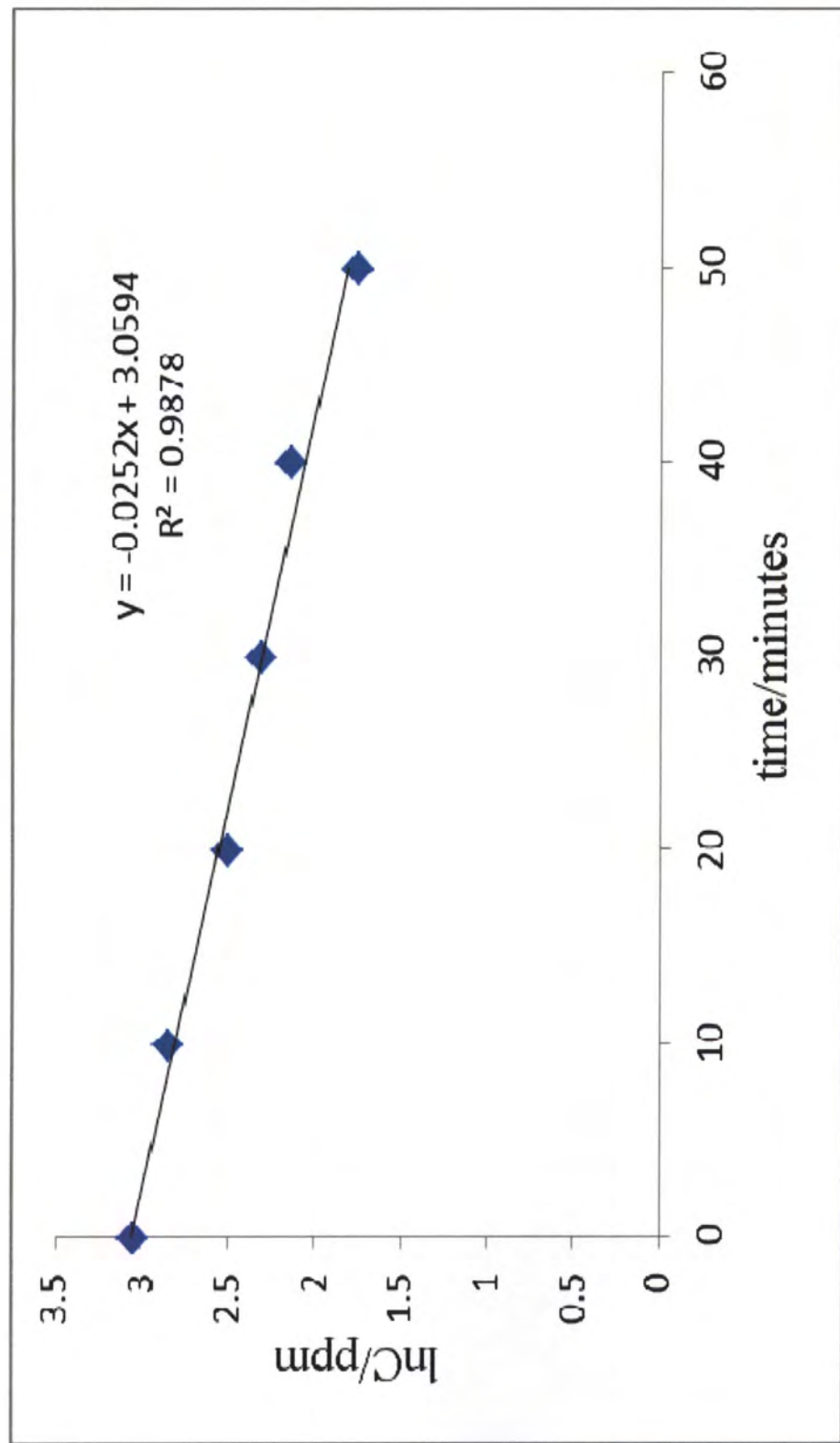
Figure 1.13 First order kinetics plot of the fumed TiO_2 mediated methylene blue decomposition. Data taken from Figure 8.

The chart shows a plot with $y = -0.0252x + 3.0594$ and $R^2 = 0.9878$, with axes labelled lnC/ppm (vertical) and time/minutes (horizontal).
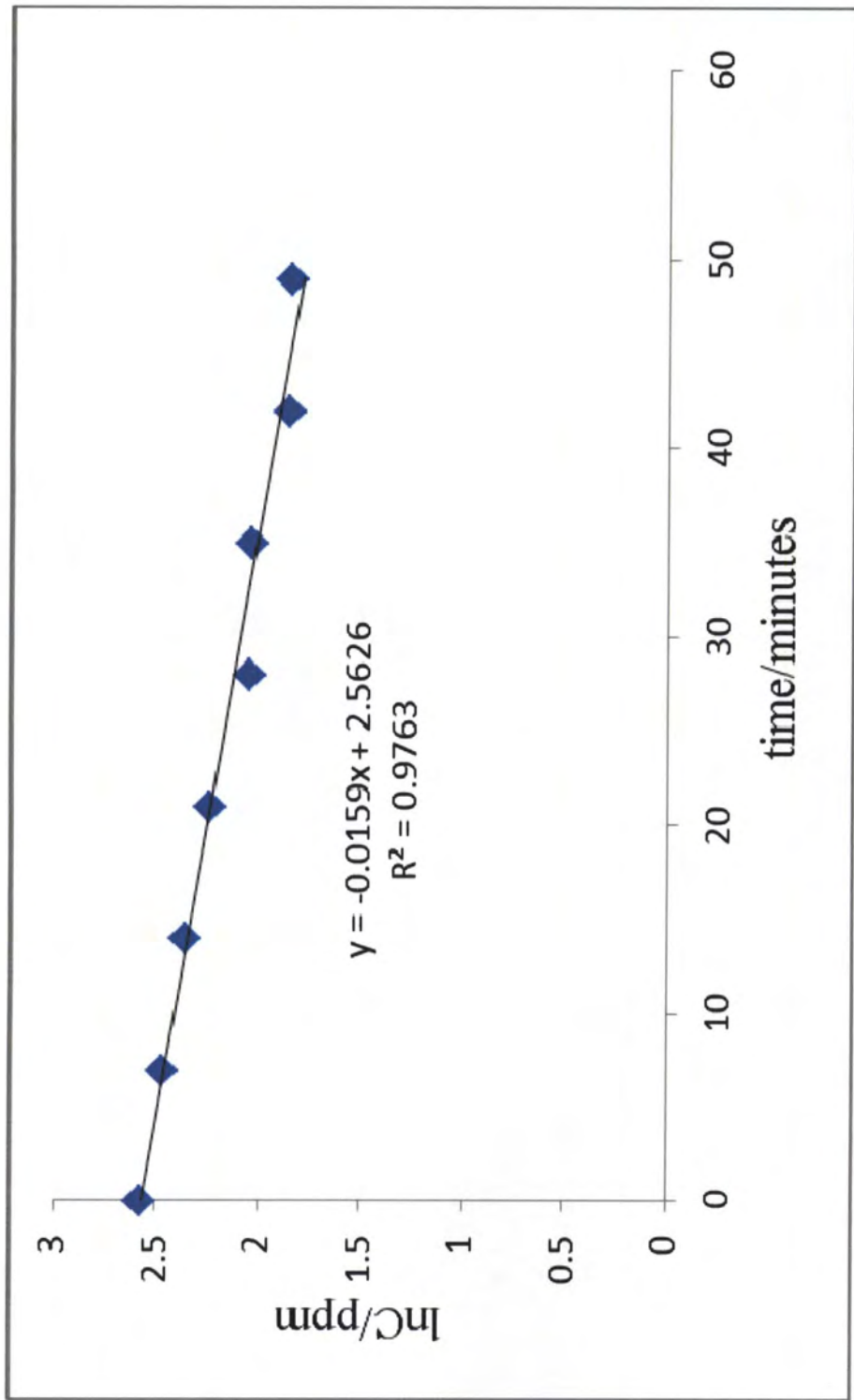
Figure 1.14 First order kinetics plot of the ST20 mediated methylene blue decomposition. Data taken from Figure 9.

37
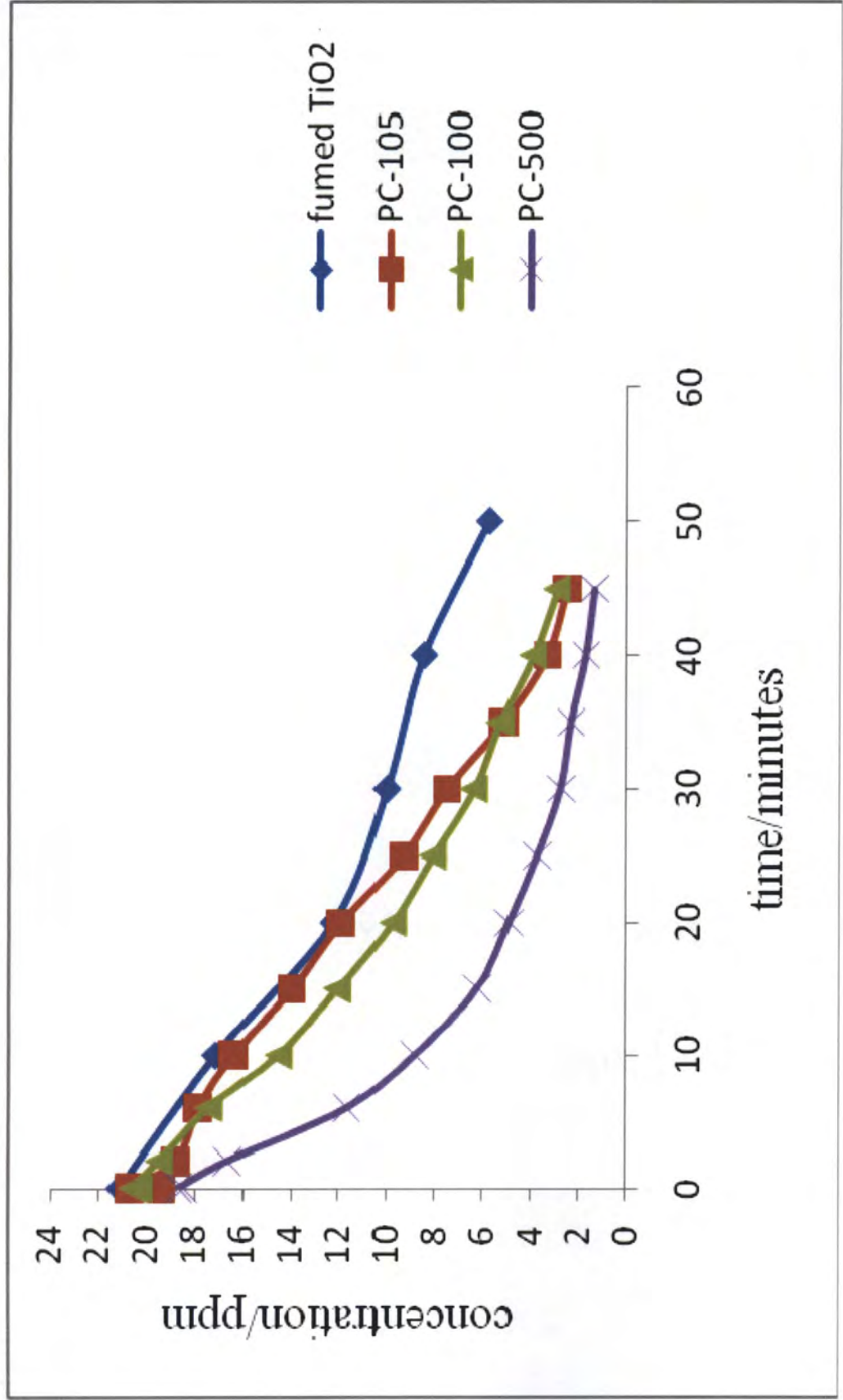
Figure 1.15 Comparison of the decomposition of methylene blue for various ultrafine TiO_2 and fumed TiO_2.

38
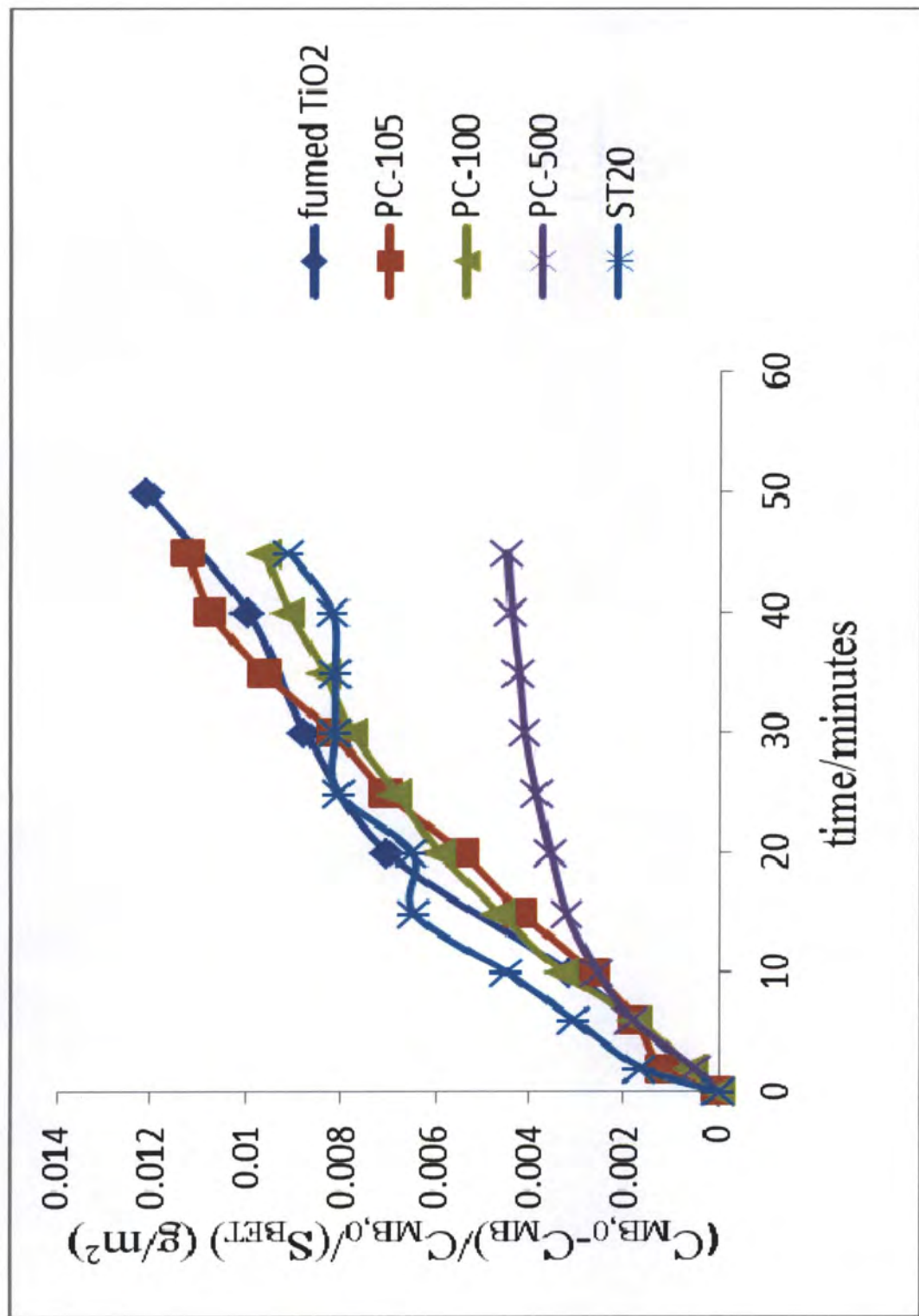
Figure 1.16 Catalytic activity of various catalysts normalized to their surface area (S_{BET}) in m^2

39
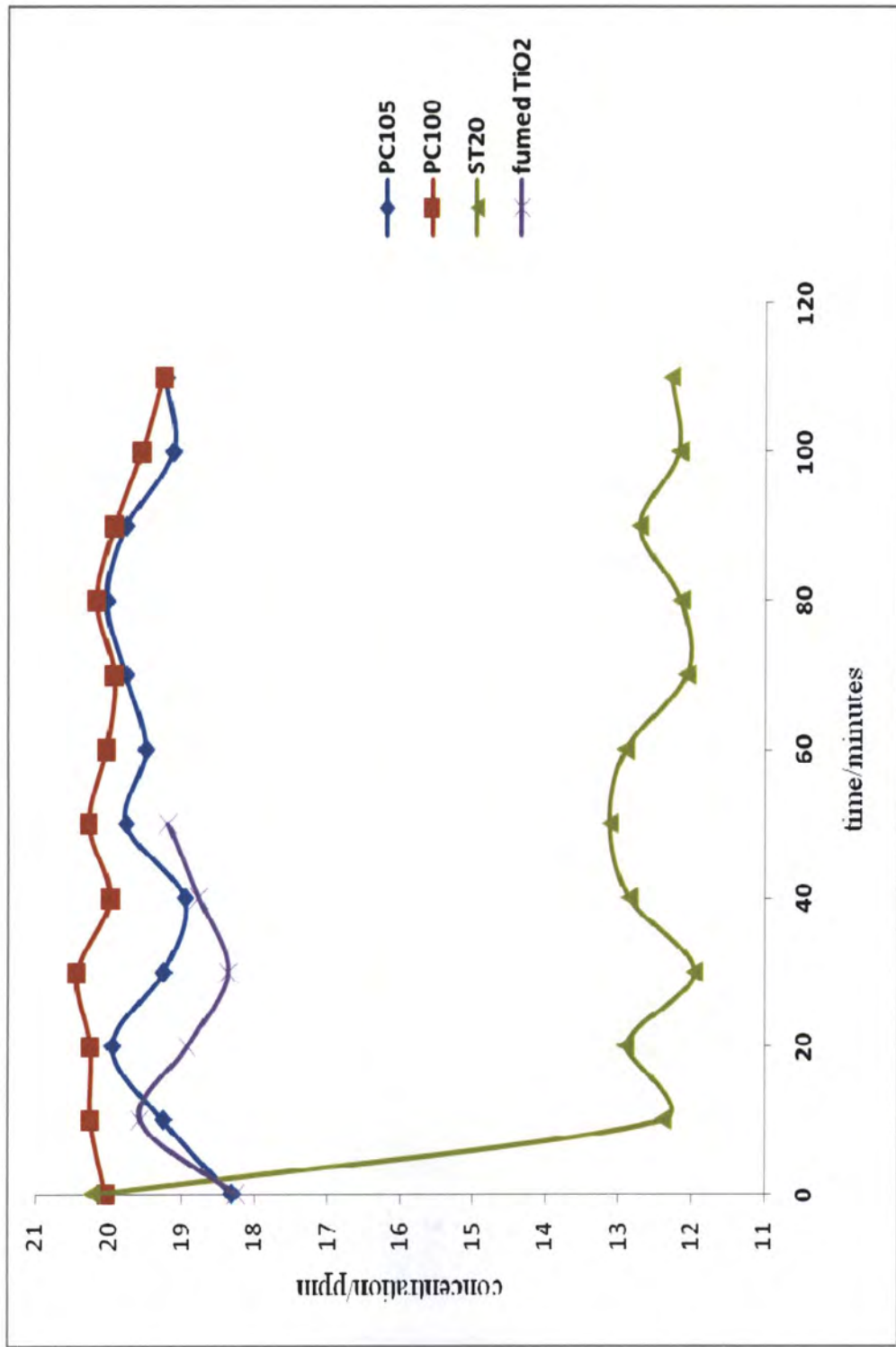
Figure 1.17 Variation of methylene blue absorbed onto the silica vs time for various TiO$_2$ catalysts

40
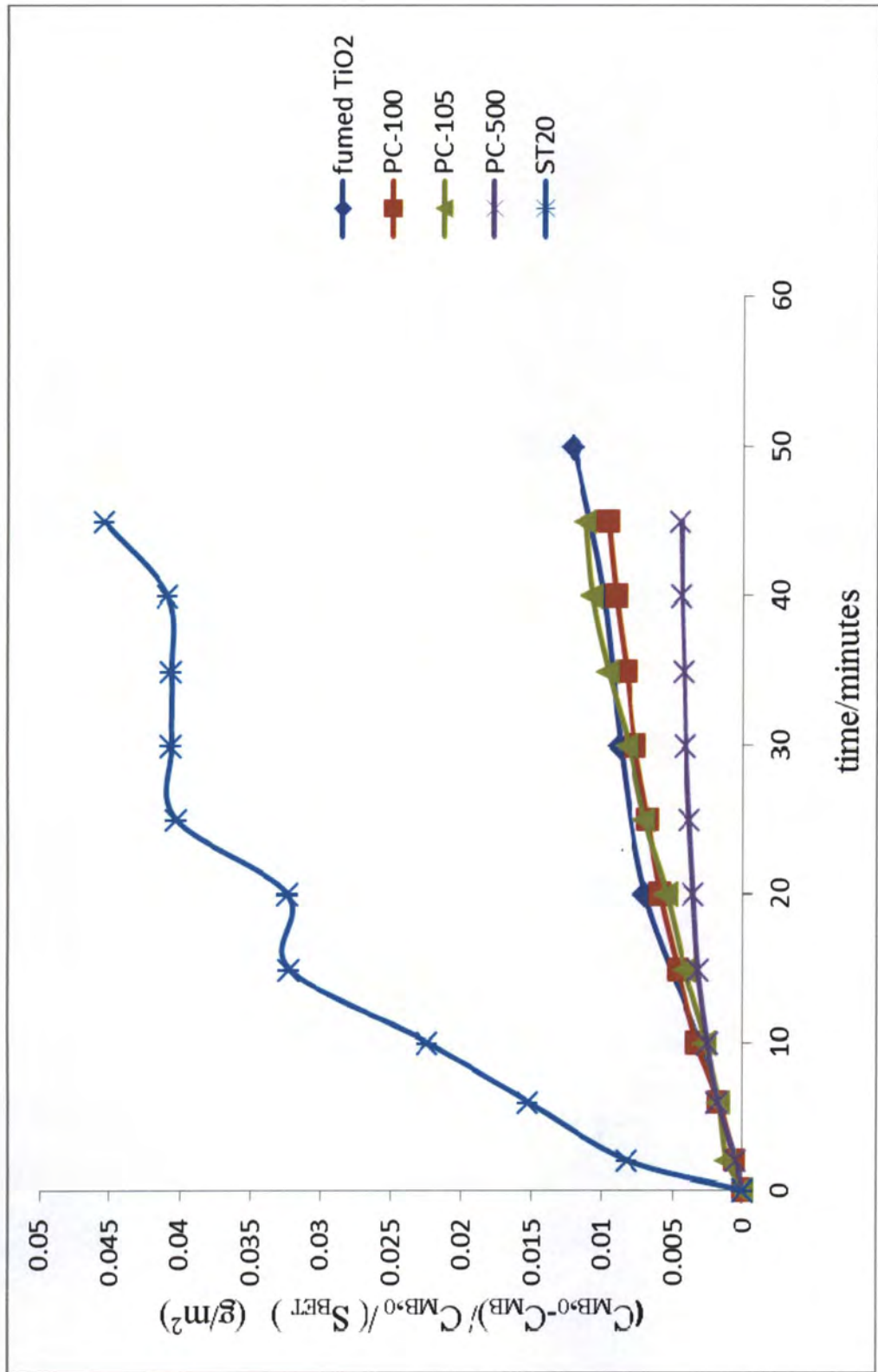
Figure 1.18 Catalytic activity of various catalysts relative to surface area of TiO_2.

41

Table 1.2 Comparison of rate constants of various TiO_2 Catalysts not normalized to specific surface area

Titania	Zero order rate constant(k)/ppm^{-1}min^{-1}	Zero order R^2	1st order rate constant(k)/min^{-1}	1st order R^2
PC-500	0.3574	0.8374	0.0578	0.992
PC-105	0.4141	0.9943	0.0455	0.9507
PC-100	0.3985	0.9678	0.0424	0.9936
Fumed TiO$_2$	0.2994	0.9628	0.0252	0.9878
ST20	0.1441	0.9619	0.0159	0.9763

Table 1.3 Comparison of 1st order rate constants of various TiO_2 Catalysts normalized to specific surface area

Titania	Rate constant(k)g/min^{-1}m^{-2}
PC-500	2.8 X 10^{-4}
PC-105	5.8 X 10^{-4}
PC-100	4.7 X 10^{-4}
Fumed TiO$_2$	4.2 X 10^{-4}
ST20	2.4 X 10^{-4}
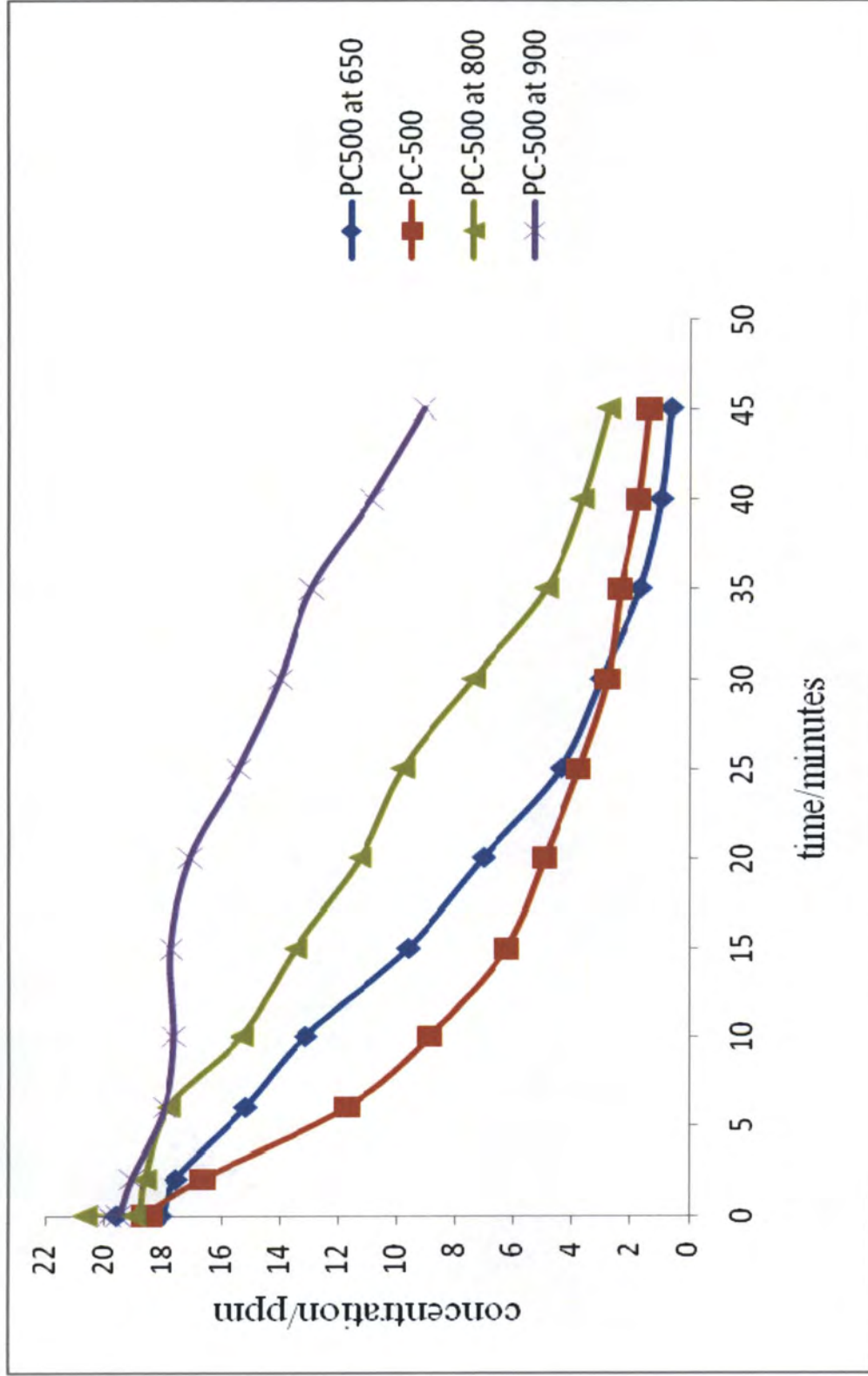
Figure 1.19 Comparison of the decomposition of methylene blue for PC-500 heated to different temperature.

1.4 CONCLUSION

The catalytic activity of these ultrafine titania and fumed titania containing nanooxides are dependent on several parameters such as particle surface area, presence of functional moieties, phase composition, content of hydroxyl groups etc. According to our data the titania with highest surface area and smallest anatase nanoparticles (PC-500) with least surface functionalities possessed the largest catalytic activity per gram based on the photodecomposition of methylene blue. On the other hand catalytic activity of various catalysts relative to per m^2 of their total surface area estimates that PC-105 showed higher catalytic activity. Catalyst with silica and titania (ST20) showed greater degradation based on the unit surface area of titania because of the strong adsorption and support by the surface silanols of silica. Heating of titania strongly affects the phase composition and other physical parameters which indeed affect the catalytic activity of the catalyst. This was observed as PC-500 heated to 650°C exhibited higher catalytic activity than PC-500 heated to higher temperatures.

1.5 References

(1) V.M. Gunko, J.P.Blitz, V.I.Zarko, V.V.Turov, E.M.Pakhlov, O.I.Oranska, E.V .Goncharuk, Y.I.Gornikov, V.S.Sergeev, T.V.Kulik, B.B.Palyanytsua, R.K.Samala *Journal of Colloid and Interface Science* 2009, 330, 125.

(2) Michael R. Hoffmann, Scot T. Martin, Wonyong Choi, and Detlef W. Bahnemannt. *Chem. Rev.* 1995, 95, 69.

(3) J.E. Hermann, *Catal. Today* 1999, 53, 115.

(4) M.I. Litter, *Appl. Catal. B: Environ.*1999, 23, 89.

(5) I. Arslan, I.A. Blacioglu, D.W. Bahnemman, *Appl. Catal. B:Environ.* 2000, 26 193.

(6) Ozdes, D.; Gundogdu, A.; Duran, C.; Senturk, H. B. *Separation Science and Technology* 2010, 45, 2076.

(7) Boer, K W. *Survey of Semiconductor Physics;* Van Nostrand Reinhold: New York, 1990; p 249.

(8) W.A.Zeltner,D.T,Tompkin, Ashrae *Transactions, vol. III, American Society of Heating and Air-Conditioning Engineers Inc.,* 2005, part 2, p. 532.

(9) J.Zhao, X. Yang, *Build. Environ.* 2003, 38, 645.

(10) A. Fujishima, T.N. Rao, D.A. Tryk, *J. Photochem. Photobiol. C* 2000, 1, 1.

(11) H.Liu, X. Ye, Z. Lian, Y. Wen, W. Shangguan, *Res. Chem. Intermed.* 2006, 32, 9.

(12) Ireland, J. C.; Klostermann, P.; Rice, E. W.; Clark, R. M. *Appl. Environ. Microbiol.* 1993, 59, 1668.

(13) Sjogren, J. C.; Sierka, R. A. *Appl. Enuiron. Microbiol.* 1994, 60, 344.

(14) Cai, R. X.; Kubota, Y.; Shuin, T.; *Sakai,* H.; Hashimoto, K; Fujishima, A. *Cancer Res.* 1992, 52, 2346.

(15) Cai, R.; Hashimoto, K.; Kubota, Y.; Fujishima, A. *Chem. Lett.* 1992, 427.

(16) Suzuki, K. In *Photocatalytic Purification and Treatment of Water and Air;* Ollis, D. F., Al-Ekabi, H., Eds.; *Elsevier: Amsterdam*, 1993.

[17] K.E. Karakitsou, X. Verykios, *J. Phys. Chem.* 1993, 97, 1184.

(18) S. Tunesi, M. Anderson, *J. Phys. Chem.* 1991, 95, 3399.

(19) C. Kormann, D.W. Brahnemann, M.R. Hoffman, *Environ. Sci. Technol.* 1991, 25, 494.

(20) R. Gomez, T. Lopez, E. Ortiz-Islas, J. Navorette, E. Sanchez, F. Tzocampanztz, X. Bokhimi, *J. Mol. Catal.* A 2003, 193, 217.

(21) G. Colon, M.C. Hidalgo, J.A. Navio, *Appl. Catal.* B 2003, 45, 39.

(22) S.K. Samantaray, P. Mohaptra, K. Parida, *J. Mol. Catal.* A 2003, 198, 277.

(23) M.V. Rao, K. Rajeshwar, V.R. Vernaker, J. Dubow, *J. Phys. Chem.* 1980, 84, 1987.

(24) S. Nishimoto, B. Ohtani, H. Kajiwara, T. Kagiya, *J. Chem. Soc. Faraday Trans.* 81 1985, 81, 61.

(25) P.F. Ollis, H. Al-Ekabi (Eds.), Photocatalytic Purification and Treatment of Water and Air, *Elsevier*, New York, 1993, pp. 169.

(26) V.M. Gun'ko, V.I. Zarko, R. Leboda, E. Chibowski, *Adv. Colloid Interface Sci.* 2001, 91, 1.

(27) V.M. Gun'ko, I.F. Mironyuk, V.I. Zarko, E.F. Voronin, V.V. Turov, E.M. Pakhlov, E.V. Goncharuk, Yu.M. Nychiporuk, T.V. Kulik, B.B. Palyanytsya, S.V. Pakhovchishin, N.N. Vlasova, P.P. Gorbik, O.A. Mishchuk, A.A. Chuiko, J.Skubiszewska-Zi̦eba, W. Janusz, A.V. Turov, R. Leboda, *J. Colloid Interface Sci.* 2005, 289, 427.

(28) V.M. Gun'ko, Y.M. Nychiporuk, V.I. Zarko, E.V. Goncharuk, O.A. Mishchuk, R. Leboda, J. Skubiszewska-Zi̦eba, E. Skwarek, W. Janusz, G.R. Yurchenko, V.D. Osovskii,

Y.G. Ptushinskii, V.V. Turov, P.P. Gorbik, J.P. Blitz, K. Gude, *Appl. Surf.Sci.* 2007, 253, 3215.

(29) V.M. Gun'ko, J.P. Blitz, K. Gude, V.I. Zarko, E.V. Goncharuk, Y.M. Nychiporuk, R. Leboda, J. Skubiszewska-Zi.eba, V.D. Osovskii, Y.G. Ptushinskii, O.A. Mishchuk, S.V. Pakhovchishin, P.P. Gorbik, *J. Colloid Interface Sci.* 2007, 314 (1), 119.

(30) V.M. Gun'ko, J. Skubiszewska-Zieba, R. Leboda, K.N. Khomenko, O.A. Kazakova, M.O. Povazhnyak, I.F. Mironyuk, *J. Colloid Interface Sci.* 2004, 269, 403.

(31) V.M. Gun'ko, V.I. Zarko, V.V. Turov, R. Leboda, E. Chibowski, *Langmuir* 1999, 15, 5694.

Chapter 2

Spatial distribution of silica surface groups using a tethered amine catalyst

2.1.1 Introduction

High surface area silicas are used in a wide variety of applications[1]. Silica is the oxide of the element silicon, in which the silicon atom is tetrahedrally coordinated with 4 oxygen atoms (SiO_4) to form the building block of silica (SiO_2). Silica is the most abundant mineral in the earth's crust and commonly found as sand or quartz, diatoms in cell walls, etc. Silica exists in two different forms: amorphous and crystalline. Crystalline silicas have a high degree of ordering in their dense structure. They are relatively inactive compared to amorphous silicas. That is, crystalline silicas are thermodynamically and kinetically more stable towards most reactants. Crystalline silica occurs in three forms: quartz, tridymite and cristobalite. Amorphous silicas can be synthetically prepared to give a very high surface area due to their porosity and/or very small particle size. Amorphous silica can be fabricated into different shapes like fibres, gels etc for different uses. The various physical properties like specific surface area, pore size, pore volume, and particle size can be controlled during the manufacturing process. Based on their increased reactivity, amorphous silicas are in general of most interest to chemists.

Two categories of synthetic amorphous silicas are silica gels and pyrogenic silicas. In general silica gels are prepared using solution processes giving highly porous materials which are commonly used as desiccants. Pyrogenic or fumed silicas are commonly prepared by flame oxidation of $SiCl_4$ to give spherical, nanometer sized nonporous primary particles. The very high

surface areas of these materials are solely determined by the particle size; that is the smaller the primary particle the larger the surface area. Sizes of 5-10 nm are typical for high surface area pyrogenic silicas. The primary particles agglomerate into chain or branch like structures as a result of hydrogen bonding of surface groups to form tertiary particles resulting in bulk porosity. These materials are often used as thickening or anticaking agents.

2.1.2 Surface Hydoxyl Groups

Hydroxyl groups at the surface of silica give rise to their reactivity. The number of hydroxyl groups per nm^2 (α_{OH}) is termed as the silanol number of the silica. Zhuravlev[2] compiled an impressive amount of work and found that for silica gels the average α_{OH} is 4.5. The silanol number represents surface reactivity of the silica which depends on the origin of the silica. Chemical methods and physical methods were used to characterize the silanols. Silanol groups can be divided based on nature, multiplicity and type of association into isolated, geminal and vicinal (figure 2.1). The surface silanols are the main centers for the adsorption and reaction of different species. These silanol groups may condense to form siloxane bonds under different conditions.
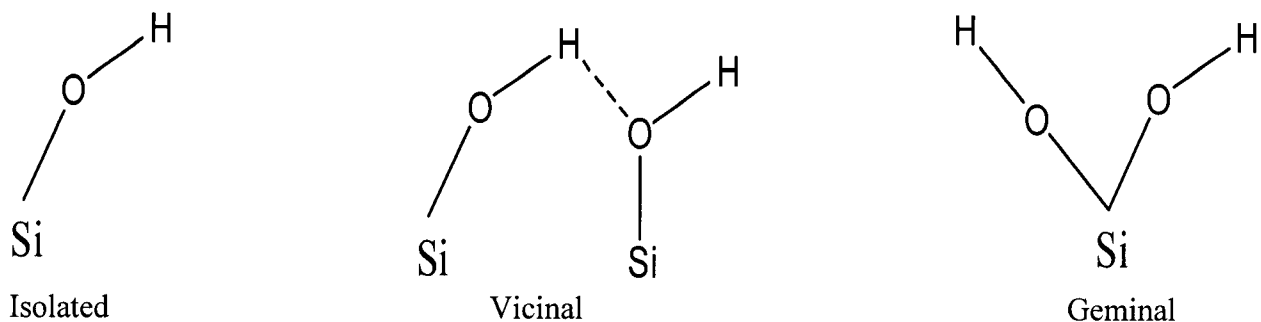
Figure 2.1 The three types of silanols that exist on silica.

49

The three types of silanols exhibit different reactivities. While isolated and germinal silianols are considered to be quite reactive, vicinal or hydrogen bonded silanols are less so.

2.1.3 Dehydration and dehydroxylation

The surface of amorphous silica consists of different types of hydroxyl groups. On exposing it to the water vapor the surface is totally hydroxylated. This was achieved by the absorption of water physically by hydrogen bonding. Multilayer of physisorbed water can be also formed under increases partial pressures. It was experimentally determined that for a non-porous silica heating at 373 K for a certain period of time removes all physisorbed water. By dehydration, temperature plays a main role as increase in temperature may lead to dehydroxylation as shown in Fig 2.2. Dehydroxylation is condensation of hydroxyl groups to form siloxane bonds. This temperature of dehydration mainly depends on porosity, surface area, pore volume and other morphological characteristics of the silica.
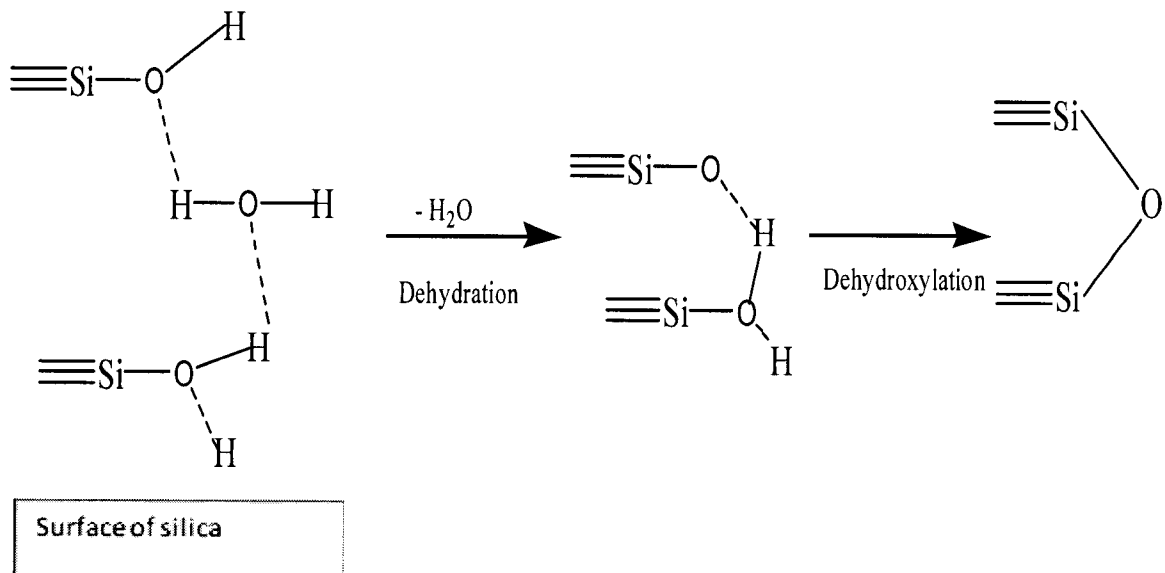
Figure 2.2 Dehydration and Dehydroxylation of silica

2.1.4 Modification of Silica Surface with Organosilanes

Organosilane-modified silicas are functionalized silicas that have a wide variety of applications in catalysis, photonics, drug delivery etc. This chemistry provides the opportunity to put onto a silica surface mostly any organic functional group that is conceivable. This modifies the chemical nature of the surface which can thus be tuned to a given application, which includes chromatographic separations[3], immobilized enzymes[4], and tribocharging for xerography[5] to name just a few.

Organofunctional silanes consist of at least one organic functional group bonded to silicon through a nonhydroylzable Si-C bond. In the same molecule there must be at least one hydrolyzable functional group; often an alkoxy group bonded to silicon (Si-OR), or a halogen bonded to silicon (Si-X). The hydrolyzable group will generally hydrolyze to form a silanol on the organosilane, which can then undergo a condensation reaction with a silica silanol to form the surface modified material as shown in Fig 2.3.

$$R_3 - Si - X \ + \ H_2O \longrightarrow R_3 - Si - OH$$

$$Si(s) - OH + HO - Si - R_3 \longrightarrow Si(s) - O - Si - R_3 + H_2O$$
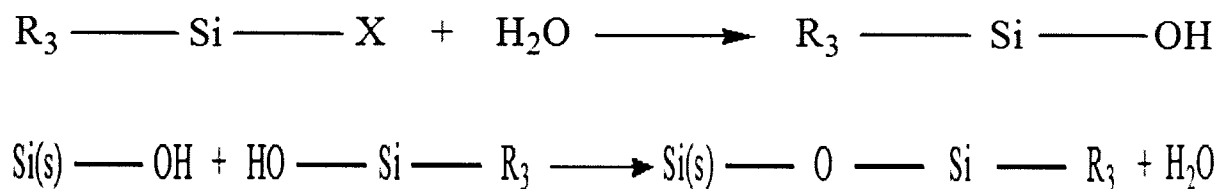
Figure 2.3 Hydrolysis and condensation of an organofunctional silane with a silica surface.

Aminofunctional silanes have long been used as coupling agents to bond two solids together in rubber technology[6]. It was found that aminosilanes exhibit unusually high reactivity. In the late 1980s it was discovered that amines catalyze the direct condensation of unhydrolyzed silane with the silica surface[7,8]. The proposed mechanism is shown in Fig 2.4.

51
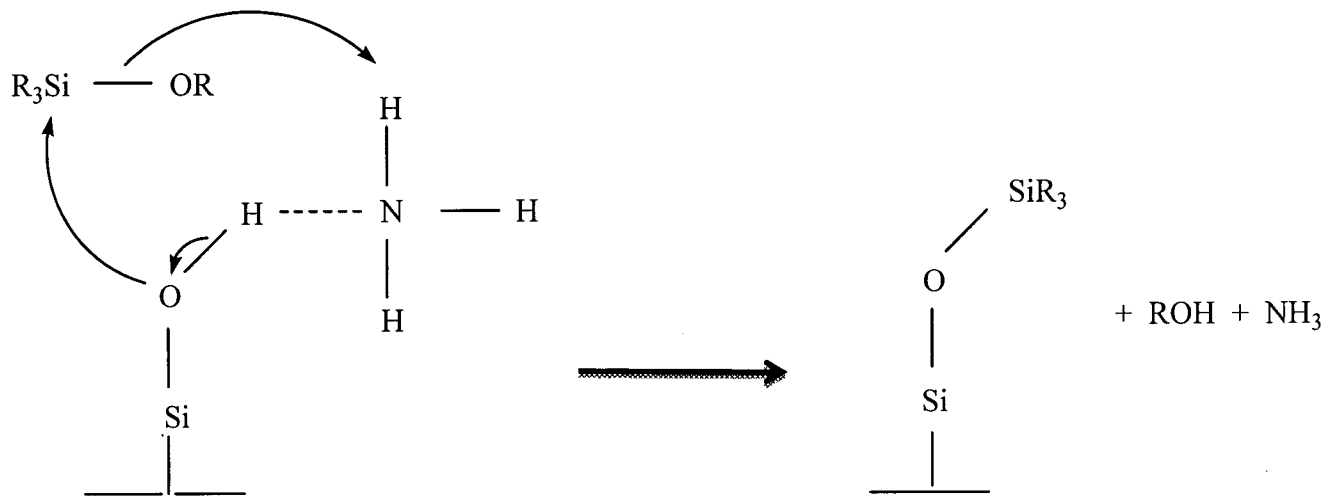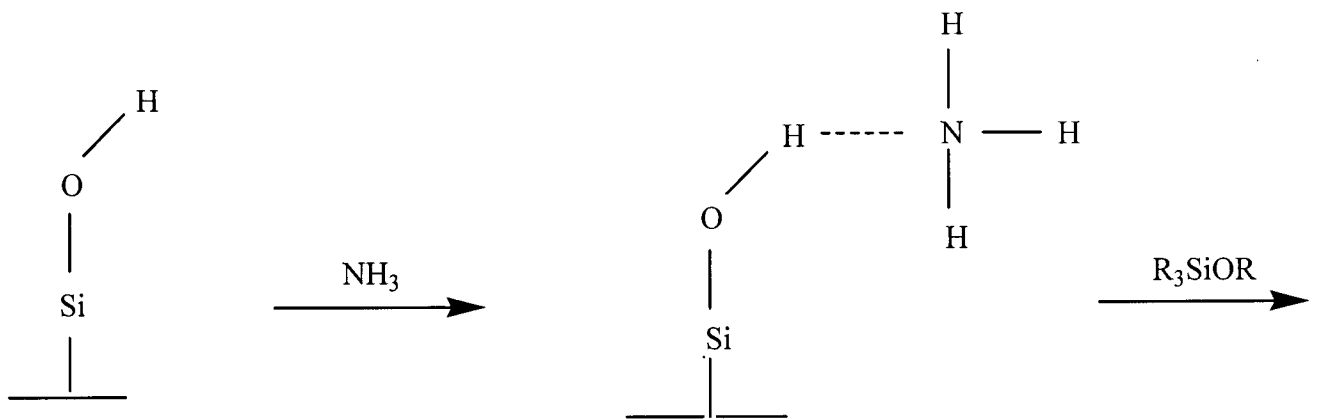
Figure 2.4 General mechanism description of amine catalysis of silylation reaction

The basic amine adsorbs to the acidic hydrogen of the surface silanol, pulling electron density towards nitrogen. This results in more electron density on the surface silanol's oxygen increasing its nucleophilicity. This oxygen attacks the electrophilic silicon, ejecting the alkoxy leaving group which forms an alcohol by abstracting the proton from the silica surface silanol. This frees the amine to adsorb on a different silanol elsewhere on the silica surface to catalyze again.

Given the above mechanism the amine is intimately involved in the transition state. If the amine is tethered to the surface it stands to reason that it could only catalyze silylation reactions where it could reach. Relatively recently there was a report[9] where a silica surface was modified with less than a stoichiometric amount of aminosilane. These researchers concluded that the aminosilane was randomly distributed about the surface; that is, it did not react in "clumps". Thus by reaction of the surface with aminosilane amount much less than α_{OH}, one could conceivably probe the number of silanols in that aminosilane's vicinity by reaction with an organosilane which will not bond unless the reaction is catalyzed by an amino group. This requirement is met with a simple alkoxyalkylsilane such as methoxytrimethylsilane (ref). The proposed experiments are to first react the silica with a small amount of an aminosilane. After washing and drying the material will be subjected to reaction with methoxytrimethylsilane. Simply by analyzing the amount of methoxytrimethylsilane reacted, the number of silanols around the aminosilane can be probed. Demonstration of this concept is the basic premise of this work.

Thus far only so called monofunctional aminosilanes, i.e.; those with one hydrolyzable group have been discussed. A limited number of experiments have been done with a trifunctional

aminosilane capable of cross-linking on the surface. The chemistry of this is shown in Fig 2.5, the consequences for this work are possibly three-fold: 1) multiple bonds to the surface may limit the "reach" of the amine group by reducing the bound molecule's flexibility; 2) oligomerization may extend the "reach" resulting in enhanced catalysis; 3) oligomerization may result in a reduction in pore size especially for the narrow pore silica gel.

To characterize the silicas carbon analysis was primarily used. Secondarily FTIR was used for fumed silica, for which this technique is readily accessible, to confirm the presence of amine functional groups and reaction of some non-hydrogen bonded silanols.

$$R \!-\!\!-\! Si \!-\!\!-\! X_3 \ + \ 3H_2O \ \longrightarrow \ R \!-\!\!-\! Si \!-\!\!-\! (OH)_3 \ + \ 3HX$$
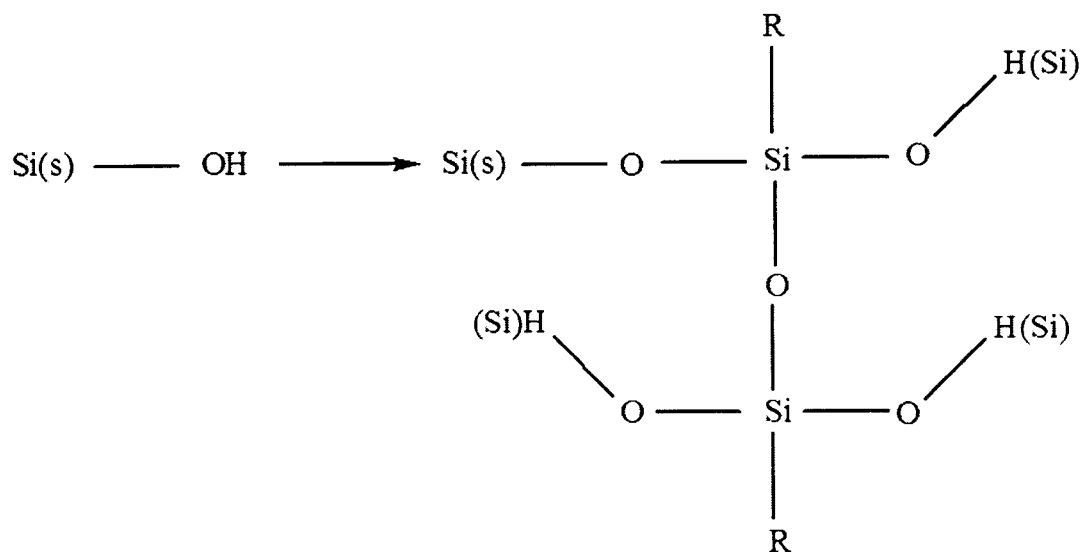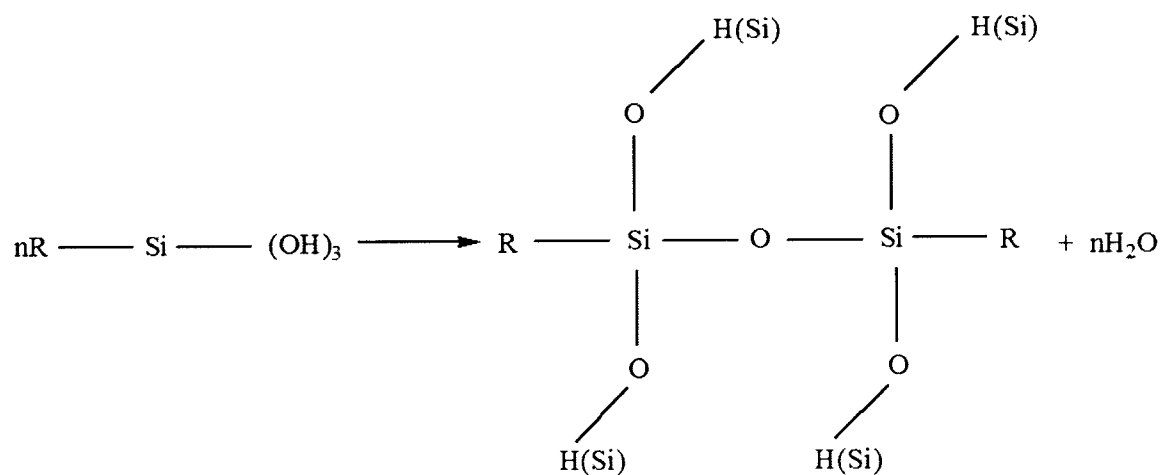
Figure 2.5 Steps involved in silica gel modification with organosilane from aqueous solution and

its oligomerization

55

2.1.5 Specific surface area (S$_{BET}$)

Specific surface area of a porous solid is the total surface area of a solid which includes the sum of internal and external areas. The external surface (S$_e$) determines the geometric surface whereas internal surface (S$_i$) determines the surface area of the pore walls. Gas adsorptions are used to characterize the surface properties of the solid. Of them physisorption is mainly used for the determination of surface area and pore size distribution. Nitrogen (at 77K) is mostly commonly used adsorptive for this process. Specific surface area is calculated from the adsorption isotherms by the BET equation. The adsorption isotherms are plotted by determining the volume of gas adsorbed on the particular solid by variation of equilibrium and saturation pressures of adsorbate.

The physisorption data is used to derive surface area by Brunauer, Emmet and Teller method. BET equation is used for the determination of surface area

$$\frac{n}{n_a(p_0 - p)} = \frac{1}{n_m C} + \frac{(C-1)}{n_m C} \bullet \frac{p}{p_0}$$

Where n_a is the amount adsorbed at the relative pressure $\dfrac{p}{p_0}$

Where n$_m$ is the monolayer capacity and C is a constant that is dependent on the isotherm shape

From derivation the surface area is determined to be

$$A_{BET} = n_m . L . a_m$$

where L is Avagadro constant and a$_m$ = molecular cross-sectional area of nitrogen.

2.1.6 Pore size distributions

The pore size distribution is one of the important characteristic which affects the physical properties of the adsorbent such as adsorption capacity, adsorption kinetics, exclusion phenomenon, and adsorption competition. Pore size distribution can be determined by various methods such as mercury porosimetry, water displacement, nitrogen adsorption at 77 K, X-ray scattering, etc. For micropores the adsorption method is most commonly applied of which nitrogen adsorption at 77 K is the standard method. In this method, the samples to be analyzed are placed in the analyzer under high vacuum at 10^{-6} Torr. The system is then brought to adsorbent temperature and adsorptions are recorded in response to the pressure change. By density functional theory (DFT) the relation between pore width and pressure filling of the pores is calibrated and the pore volume is calculated. The pore size distributions are calibrated by plotting average pore diameter with respect to pore volume and surface area as shown in the experimental using custom software developed by collaborators at the Ukrainian Institute of Surface Chemistry.

Pores are the channels which communicate on the silica surface and thus increase the area of reacting sites. The IUPAC classification of the pores is given in Table 2.1.

Table 2.1 IUPAC classification of pores

Name	Pore diameter(nm)
Micropores	0-2
Mesopores	2-50
Macropores	50-7500
Megapores	>7500

2.1.7 FTIR spectroscopy

FTIR spectroscopy measures the absorption of wavelengths in the infrared region by the molecules. Functional groups are determined in the molecule by the respective peaks in the spectrum. In this work transmission spectrum was used to determine the functional groups. In transmission spectroscopy the infrared radiation passes through the sample and the amount of radiation absorbed by the sample is measured. The intensity of the spectrum depends on the path length, absorption coefficient and concentration of the sample. Transmission spectroscopy can only be accomplished with the pyrogenic silica because the nanometer sized primary particle size does not result in scattering of infrared radiation. By contrast the silica gels have particle sizes >10 μm which result in significant scatter rendering the acquisition of infrared spectra by transmission spectroscopy impossible.

2.1.8 CHN analyzer:

CHN analyzer is used to measure carbon, hydrogen and nitrogen content in organic and inorganic molecules. The samples are combusted in pure oxygen in static conditions and helium

is used for transportation of combusted products because of its inert nature and high coefficient

of thermal conductivity. The silane reacted samples were combusted in CHN analyzer to

measure the carbon, hydrogen and nitrogen content.
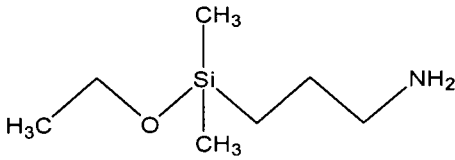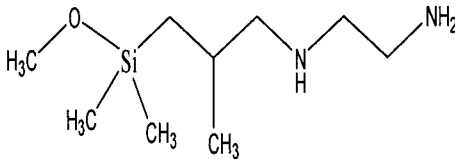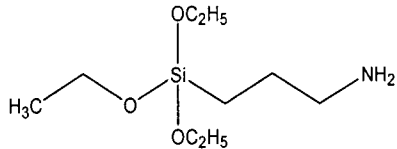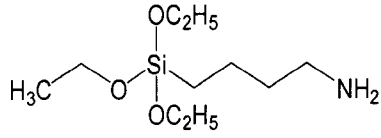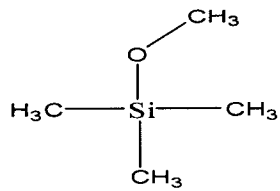
2.2 MATERIALS AND METHODS

2.2.1 MATERIALS

2.2.1.1 Silicas: The silica gel samples, HP39 "wide pore" silica gel and 200DF "narrow pore" silica gel were donated by the PQ Corporation (Philadelphia, PA, USA). Pyrogenic or fumed silica (HS-5) was donated by the Cabot Corporation (Tuscola, IL, USA).

2.2.1.2 Aminosilanes: Organofunctional silanes shown in the Table 2.2 were obtained from Gelest, Inc., Morrisville, PA, USA. These silanes were typically >98% pure and used as received.

Table 2.2 Organosilane structures and number of hydrolyzable groups

Type of Aminosilane	Structure	Number of reactive (hydrolyzable) functional groups
3-Amino propyl dimethyl ethoxy silane(APDMES)		1
N-2-Amino ethyl 3-amino isobutyl dimethyl methoxy silane(AEIDMS)		1
3-Amino propyl triethoxy silane(APTES)		3
4-Amino Butyl triethoxy silane(ABTES)		3
Trimethyl Methoxy silane		1

2.2.2 Instrumentation

2.2.2.1 FTIR spectroscopy: A Nicolet Avatar 360 FT-IR E.S.P was used to obtain absorption FTIR transmission spectra of fumed silica samples. Typically approximately 5 mg of sample was placed between a pair of NaCl windows and rotated to spread the sample. Since particles of fumed silica are very small there is little scatter of the infrared beam using this transmission technique providing quality transmission spectra.

2.2.2.2 CHN Analyzer : CHN analysis was done at the University of Illinois at Urbana Champaign microanalysis laboratory where a CE 440 CHN analyzer was used. The modified silica samples were combusted in pure oxygen under static conditions.

2.2.2.3 Nitrogen Adsorption: N_2 adsorption isotherms were done at SABIC in Baltimore, MD. A Micrometrics ASAP 2010 adsorption analyzer was utilized to obtain surface area and porosity measurements. The isotherms were recorded at 77.35 K and at p/p_0 10^{-6} to 10^{-5} where p and p_0 denote the equilibrium and saturation pressures of adsorbate. The specific surface area (S_{BET}) of the solid particles was calculated using the standard BET method. Pore size distribution of the silica was obtained with standard DFT software. The average pore volume (V_p) was calculated from nitrogen adsorption at p/p_0 is 0.33.

2.2.3 Methods

2.2.3.1 Sample preparation: All the silicas to be modified were dried at 100^0C in vacuum for a period of 2 hours for the removal of physisorbed water from the surface.

2.2.3.2 Synthesis of Aminosilane modified silicas: In all the grafting experiments of the silica 2 g of vacuum dried silica were dispersed in 60 mL of toluene and a calculated amount of

aminosilane was added. The calculation was done based on the specific surface area, silanol

number and the number of moles as shown below. The silanol[2] number for 200DF and HP39 is 4

per nm^2 while for HS-5[11] it is 3 per nm^2. The whole suspension was refluxed in toluene for a

period of 3 hours. The aminosilylated silica was recovered by vacuum filtration and washed with

100 mL of toluene to remove any traces of unreacted aminosilane for multiple times.

Calculation of amount of silane

Example: For HP39

Number of moles of SiOH per gram = 470 m^2/g X $10^{18}nm^2/m^2$

$$= 4.7 \text{ X } 10^{20} \text{ } nm^2/g \text{ X } 4 \text{ SiOH/ } nm^2$$

$$= 1.9 \text{ X } 10^{21} \text{ SiOH/g}$$

$$= 1.9 \text{ X } 10^{21} \text{ SiOH/g X } \frac{1 \text{mole}}{6.023 \text{ X } 10^{23}} = 3.12 \text{ mmol SiOH/g HP39 } SiO_2$$

Table 2.3 Amount of aminosilane added depending upon the silica characteristics.

Type of silica	Number of SiOH/nm^2	Specific surface area	Number of SiOH/g	Number of mMol SiOH/g	Amount of aminosilane per gram of silica mmol/g
HP39	4	470 m^2/g	1.9X10^{21} SiOH/g	3.12 mmol SiOH/gm	0.31
200DF	4	530 m^2/g	2.12X10^{21} SiOH/g	3.52 mmol SiOH/gm	0.35
HS-5	3	350 m^2/g	1.05 X10^{21} SiOH/g	1.74 mmol SiOH/gm	0.17

2.2.3.3 Postcuring: After reaction with the aminosilane, the functionalized silicas were dried at 100°C in vacuum for a period of 2 hours.

2.2.3.4 Catalysis of TMMS onto aminosilylated silica: To determine the extent to which an anchored aminosilane can perform amine catalysis, 1 g of aminosilane modified silica was dispersed in 30 mL of toluene and to it 5mmol of TMMS was added. The suspension was left for reaction over a period of 3 hours swirling the solution in 15 minute intervals. The TMMS catalyzed silica was recovered by filtration and washed with 100 mL of toluene for several times for removal of any traces of unreacted TMMS. The functionalized silica was then vacuum dried at 100°C for 2 hours.

2.2.3.5 Analysis: The functionalized silicas were analyzed for carbon content after reaction with the aminosilane both before and after reaction with TMMS

2.3 Results and discussion

2.3.1 Comparison of specific surface area and pore size distributions

The nitrogen adsorption isotherms of 200DF and HP39 from Figure 2.6 were analyzed using the BET equation. The specific surface areas and the average pore volumes are calculated by DFT software and included in Table 2.4. The specific surface area of fumed silica HS-5 was taken from reference 11. The porosity of HS-5 is a result of aggregation and agglomerates of the silica particles which primarily depend on the nature of the physical environment and others. As the chemical environment changes with the change in the aminosilane, the porosity may change in unexpected ways and are not taken into account for the fumed silica.

Table 2.4 Physical properties of all silicas

Type of silica	BET specific surface area(m^2/g)	Pore width(W_{KJS} nm)	Single point Pore volume (V_t CCg^{-1})
HS-5	350	Variable	Variable
HP-39	470	15.97	1.96
200DF	530	2.64	0.30

From the Figure 2.7 silica gel 200DF has mostly narrow pores with pore radii R < 2 nm and the contribution of mesopores and macropores is much less. In contrast HP39 has mostly mesoporous pores with the major peak at 2 nm < R < 20 nm and a very small percentage of micro and macropores. The pore distribution of HS-5 mostly constitutes macropores with some mesopores also present.

2.3.2 Comparison of extent of surface modification

To test whether it is possible to interpret results based on the proposed concept, that is the use of an anchored aminosilane to catalyze the reaction of nearby surface silanols, at least two requirements must be met given the approach taken here. First if TMMS is to be catalyzed with the anchored aminosilane, it must have little or no reactivity in the absence of the aminosilane. Table 2.5 shows elemental analysis data for reactions done with the three silicas exposed only to the solvent toluene, as well as for reactions in toluene slurry with dissolved TMMS and with no pre-reacted aminosilane.

These data show that in the absence of TMMS there is a background C amount of approximately 0.1 mmol/g of silica, and in the presence of TMMS a C amount of ~ 0.2 − 0.5 mmol/g. Note that given that TMMS results in a trimethylsilyl group, the number of moles of TMMS would be 3-fold less than the carbon content calculated. The background N content is an average of a negligible 0.02% N. Finally notice that these samples all have relatively high hydrogen contents, especially given hydrogen's low atomic mass. It is probable that these values are largely influenced by the silanol content of these high surface area silicas. This is supported by the fact that the fumed silica HS5 exhibits by far the lowest H content, and this material has both the lowest surface area and the fewest silanols per unit surface area[11].

Table 2.5 Blank reaction data.

Sample	%C	%C variance	%H	%N	%N variance	Avg %C	mmol C/g sample
HS5 + Toluene	0.13 / 0.16	0.00045	0.22 / 0.09	0.03 / 0.02	0.00005	0.14_5	0.12_1
200DF+ Toluene	0.11 / 0.08	0.00045	0.41 / 0.48	0.02 / 0.02	0	0.09_5	0.079
HP39+ Toluene	0.11 / 0.1	0.00005	0.39 / 0.25	0.02 / 0.04	0.0002	0.10_5	0.087
HS5 + TMMS	0.48 / 0.42	0.0018	0.32 / 0.27	0.02 / 0.01	0.00005	0.45	0.37_5
200DF+ TMMS	0.21 / 0.17	0.0008	0.34 / 0.41	0.02 / 0	0.0002	0.19	0.15_8
HP39+ TMMS	0.45 / 0.44	0.00005	0.35 / 0.33	0.01 / 0	0.00005	0.44_5	0.37_1

Reaction of aminosilanes on the silica is confirmed by comparing the IR spectrum of the fumed silica before and after the reaction. By comparing the silanol peak 3750 cm-1 and the siloxane peak 1860 cm-1 from the Figure 2.8 and 2.9 it was clear that after the aminosilane reaction there is a rise in siloxane peak and fall of silanol. The rise of CH stretching peaks at 2920 cm-1 from the aminosilane reacted silica are clearly evident after the aminosilane catalysis.

Table 2.6, 2.8 and 2.10 give the elemental analysis of the different aminosilane modified silicas. A second requirement for these experiments to yield meaningful results is that after the aminosilane is reacted to the silica, it must remain on the surface through the subsequent TMMS reaction. It can be seen that this requirement is met from the HP39 (wide pore silica gel) data (Table 2.7) with the four aminosilanes tested. Note that the nitrogen content is unchanged (within experimental error) before and after TMMS reaction, suggesting no change in aminosilane content. Compared to the change in carbon content, which increases significantly after TMMS reaction, these results are in agreement with what one would expect for an aminosilane anchored to the surface catalyzing the reaction of TMMS with nearby surface silanol(s). These reassuring data trends exist also for the other silicas 200DF (narrow pore) and HS5 (fumed) samples shown in Tables 2.9 and 2.11.

The reaction of TMMS is also confirmed by the comparison of the silanol to siloxane before and after TMMS catalysis. Table 2.12 includes the data regarding the silanol to silxoane ratio on HS-5 silica. The 3750 cm^{-1} silanol peak and 1860 cm^{-1} siloxane peaks are used to calculate the peak areas to compare aminosilane and TMMS reaction. The area is calculated by selecting the required peak and using the peak area tool selected the left and right boundaries on X-axis. Similarly vertical lines are drawn limiting the region and a baseline appears through the

lowest data points and the area of the peak is determined. From the Table 2.12 ratio of silanol to siloxane ratio decreases after the TMMS catalysis as the number the TMMS molecules are catalyzed onto the silica the same number of silanols convert into siloxane bonds. The quantitative data of these ratio makes rough sense except for aminosilane APDMES where the ratio increases after TMMS catalysis. However when the ratio was compared to the blank reaction ratio involving only Tolune or TMMS, the ratio for all samples after aminosilane decreased and it further decreased for all samples after TMMS reaction except APDMES.

An implicit assumption related to the carbon data also exists for the trifunctional aminosilanes APTES and ABTES. In calculating the increase in carbon content before and after TMMS reaction, it is assumed that all of that increase comes from the trimethylsilyl groups of TMMS. This number does not take into account the possibility of the loss of ethoxy groups on the aminosilane during the TMMS reaction. Thus the calculated increase in the carbon content is an upper limit. However it is believed that this is unlikely to be a large factor since all reactions, including the TMMS reaction, is done largely in the absence of water limiting the role of hydrolysis. The argument made here is that all or nearly all ethoxy group loss occurs during the aminosilane reaction when these molecules react with the surface. Additional loss seems unlikely.

Table 2.6 Elemental analysis of different aminosilane reacted wide pore silica (HP39)

sample	%C	%H	%N	Avg %C	%C variance	Avg %N	%N variance	mmol C/g sample	mmol N/g sample
HP39 + APTES	1.35 1.34	0.45 0.51	0.42 0.42	1.345	0.00005	0.420	0.00180	1.120	0.300
HP39 + ABTES	1.68 1.75	0.61 0.53	0.43 0.44	1.715	0.00245	0.435	0.00005	1.428	0.310
HP39 + AEIDMS	3.03 3.08	0.73 0.82	0.85 0.86	3.055	0.00125	0.855	0.00005	2.544	0.610
HP39 + APDMES	1.77 1.73	0.27 0.24	0.31 0.31	1.750	0.0008	0.310	0	1.457	0.221

Table 2.7 Elemental analysis of TMMS catalyzed different aminosilane reacted wide pore silica (HP39)

sample	%C	%H	%N	Avg %C	%C variance	Avg %N	%N variance	Increase %C from TMMS	Change in %N
HP39 + APTES + TMMS	2.56	0.76	0.43	2.555	0.00005	0.430	0	1.210	0.01
	2.55	0.7	0.43						
HP39 + ABTES + TMMS	3.24	0.72	0.47	3.075	0.05445	0.445	0.00125	1.360	0.01
	2.91	0.72	0.42						
HP39 + AEIDMS + TMMS	3.7	0.95	0.85	3.700	0	0.845	0.00005	0.645	-0.01
	3.7	0.9	0.84						
HP39 + APDMES + TMMS	2.79	0.46	0.34	2.780	0.00020	0.340	0.00020	1.030	0.03
	2.77	0.46	0.34						

Table 2.8 Elemental analysis of different aminosilane reacted narrow pore silica (200DF)

sample	%C	%H	%N	Avg %C	%C variance	Avg %N	%N variance	mmol C/g sample	mmol N/g sample
200DF + APTES	2.07 1.64	0.63 0.63	0.50 0.43	1.855	0.09245	0.465	0.00245	1.54_5	0.33_2
200DF + ABTES	2.06 2.04	0.91 0.85	0.44 0.45	2.050	0.00020	0.445	0.00005	1.70_7	0.31_8
200DF + AEIDMS	3.26 3.12	0.77 0.66	0.82 0.84	3.190	0.00980	0.830	0.00020	2.65_6	0.59_2
200DF + APDMES	2.17 2.09	0.70 0.70	0.44 0.41	2.130	0.00320	0.425	0.00045	1.77_4	0.30_3

Table 2.9 Elemental analysis of TMMS catalyzed different aminosilane reacted narrow pore silica (200DF)

sample	%C	%H	%N	Avg %C	%C variance	Avg %N	%N variance	Increase %C from TMMS	Change in %N
200DF + APTES + TMMS	2.47 2.58	0.84 0.75	0.45 0.43	2.525	0.00605	0.440	0.00020	0.670	-0.025
200DF + ABTES + TMMS	2.87 3.02	0.9 1.01	0.49 0.49	2.945	0.01125	0.490	0	0.895	0.045
200DF + AEIDMS + TMMS	4.05 3.98	0.75 0.69	0.88 0.87	4.015	0.00245	0.875	0.00005	0.825	0.045
200DF + APDMES + TMMS	2.8 2.72	0.84 0.78	0.47 0.45	2.760	0.0032	0.460	0.00020	0.63	0.035

Table 2.10 Elemental analysis of different aminosilane reacted pyrogenic silica (HS-5)

sample	%C	%H	%N	Avg %C	%C variance	Avg %N	%N variance	mmol C/g sample	mmol N/g sample
HS-5 + APTES	0.93 0.86	0.24 0.18	0.25 0.24	0.89_5	0.00245	0.24_5	0.00005	0.74_5	0.17_5
HS-5 + ABTES	1.14 1.27	0.21 0.18	0.24 0.26	1.20_5	0.00845	0.25_0	0.00020	1.00_3	0.17_8
HS-5 + AEIDMS	1.7 1.8	0.37 0.39	0.47 0.46	1.75_0	0.005	0.46_5	0.00005	1.45_7	0.33_2
HS-5 + APDMES	1.24 1.26	0.2 0.1	0.15 0.20	1.25_0	0.0002	0.17_5	0.00125	1.04_1	0.12_5

Table 2.11 Elemental analysis of TMMS catalyzed different aminosilane reacted pyrogenic silica (HS-5)

sample	%C	%H	%N	Avg %C	%C variance	Avg %N	%N variance	Increase %C from TMMS	Change in %N
HS-5 + APTES + TMMS	1.73 / 1.67	0.34 / 0.34	0.25 / 0.24	1.700	0.00180	0.245	0.00005	0.80_5	0
HS-5 + ABTES + TMMS	1.9 / 1.87	0.41 / 0.32	0.23 / 0.24	1.885	0.00045	0.235	0.00005	0.68_0	-0.015
HS-5 + AEIDMS + TMMS	2.44 / 2.36	0.54 / 0.50	0.47 / 0.45	2.400	0.00405	0.460	0.00020	0.65_0	-0.005
HS-5 + APDMES + TMMS	2.09 / 1.99	0.35 / 0.35	0.24 / 0.24	2.040	0.00500	0.240	0	0.79_0	0.065

Table 2.12 IR spectra peaks and areas of HS-5 silica

Sample	peaks	area	Ratio of silanol to siloxane peak areas
HS-5 + APTES	3745	0.059	0.106
	1834	0.553	
HS-5 + APTES + TMMS	3745	0.076	0.039
	1834	1.941	
HS-5 + ABTES	3745	0.055	0.108
	1837	0.510	
HS-5 + ABTES + TMMS	3745	0.080	0.080
	1837	0.997	
HS-5 + AEIDMS	3745	0.080	0.133
	1834	0.599	
HS-5 + AEIDMS + TMMS	3745	0.117	0.0982
	1834	1.191	
HS-5 + APDMES	3745	0.091	0.0728
	1837	1.250	
HS-5+ APDMES + TMMS	3739	0.420	0.2730
	1837	1.538	
HS-5 + Toluene	3751	2.084	1.352
	1832	1.541	
HS-5 + TMMS	3751	1.126	0.6120
	1922	1.840	

Results from analysis of the data in Table 2.6 – 2.11 are shown in Tables 2.13 – 2.15 for HP39,

200DF, and HS5 silicas; respectively.

Table 2.13 HP39 data analysis from raw data in Table 6 & 7.

Aminosilane	mmol aminosilane/g SiO_2	mmol C/g silica from TMMS	mmol TMMS/g SiO_2	SiOH reacted per aminosilane
APTES	0.30_0	1.00_7	0.33_6	1.12_0
ABTES	0.31_0	1.13_2	0.37_7	1.21_6
AEIDMS	0.30_5	0.53_7	0.17_9	0.58_7
APDMES	0.22_1	0.85_8	0.28_6	1.29_2

Table 2.14 200DF data analysis from raw data in Table 8 & 9.

	mmol aminosilane/g SiO_2	mmol C/g silica from TMMS	mmol TMMS/g SiO_2	SiOH reacted per aminosilane
APTES	0.33_2	0.55_8	0.18_6	0.56_0
ABTES	0.31_8	0.74_5	0.24_8	0.78_2
AEIDMS	0.29_6	0.68_7	0.22_9	0.77_3
APDMES	0.15_2	0.52_5	0.17_5	1.15_3

Table 2.15 HS5 data analysis from raw data in Table 10 & 11.

Aminosilane	mmol aminosilane/g SiO_2	mmol C/g silica from TMMS	mmol TMMS/g SiO_2	SiOH reacted per aminosilane
APTES	0.17_5	0.67_0	0.22_3	1.27_8
ABTES	0.17_8	0.56_6	0.18_9	1.05_8
AEIDMS	0.16_6	0.54_1	0.18_0	1.08_7
APDMES	0.12_5	0.65_8	0.21_9	1.75_5

79

As an explanation of the data in Tables 2.13 – 2.15, the second column of mmol aminosilane is taken from the corresponding Table 2.6, 2.8 and 2.10 of mmol N/g silica, except for AEIDMS. Since this silane has 2 amine groups, that number is divided by 2. The next column is derived from the calculated increase in % C in the corresponding earlier table. The third column takes the 2nd column and divides by three since there are three carbons per trimethylsilyl group from TMMS bound to the surface. This column has units of TMMS/g SiO_2, however it is not normalized to the amount of aminosilane per gram, so its usefulness is limited. To obtain the last column it is assumed that each TMMS bonds to one silanol, divide that by the aminosilane/g value in the first column of data. This last column potentially provides some molecular level insight into what is occurring at the silica surface.

It is impossible to analyze the data as given without having some estimate of the uncertainty of the numbers, especially the uncertainty of the number in the last column of Tables 2.13–2.15. In order to calculate the uncertainty of the ratio of the number of silanols reacted by TMMS per aminosilane bonded to the silica, an uncertainty estimate of the %C and %N data had to be obtained. It was decided to calculate a pooled standard deviation of all analyses grouped by silica gel type, i.e.; HP39, 200DF, and HS5. While there are just two analyses per sample, with the 2 blank sets of data plus 8 data sets from organosilane reactions for each silica, this provides a reasonable amount of data for the pooled standard deviation calculation. Using the calculated standard deviation from the pooled data for each silica with respect to the elemental analysis (%C, %N) results, standard methods of uncertainty propagation were used to find the standard deviation of the final result (SiOH reacted/aminosilane bonded). Results of this analysis are given in Table 2.16, 2.17 and 2.18.

Calculation of standard deviation for SiOH reacted/aminosilane:

Example for 200DF + APDMES + TMMS =

Sum of pooled %C variance from Table 4 and 5 for 200DF =

$$s_p^2 = \frac{\sum_{i=1}^{k}((n_i - 1)s_i^2)}{\sum_{i=1}^{k}(n_i - 1)}$$

$$= \frac{(2-1)(0.0045) + (2-1)(0.0008) \ldots\ldots.(2-1)(0.0032)}{(2-1) + (2-1)\ldots\ldots.(2-1)}$$

$$= \frac{0.12985}{5}$$

$$= 0.02597$$

pooled standard deviation of %C for 200DF $= \sqrt{s_p^2} = \sqrt{0.02597} = 0.161$

Using %N variance from Table 4 & 5 the Pooled standard deviation of %N for 200DF = 0.0276

Absolute uncertainty of %N for 200DF = 0.0276

Relative uncertainty of mmol aminosilane APDMES $= \dfrac{Absolute\ uncertanity\ of\ \%N}{magnitude\ of\ measurement}$

$$= \frac{0.027}{0.465}$$

$$= 0.059$$

The %C increase from TMMS is obtained from subtraction of 2 carbon numbers so the uncertainty propagation uses absolute standard deviation values.

Absolute %C increase uncertainty $= \sqrt{a^2 + b^2}$

$$= \sqrt{(0.161)^2 + (0.161)^2}$$

$$= 0.227$$

Ultimately the relative uncertainty of %C/g increase which is same as R.U. of TMMS/g which is same as R.U. SiOH reacted/g. Calculation below for APDMES silane.

$$\text{Relative uncertainty of} \frac{\text{TMMS}}{\text{g}} \text{catalyzed by APDMES} = \frac{0.227}{0.63} = 0.362$$

Relative uncertainty of the ratio of the number of silanols reacted by TMMS per aminosilane bonded to the silica for APDMES = 0.367

Absolute S.D. above obtained by multiplying R.U. Silanol/aminosilane by the corresponding original ratio = 0.362 X 1.153 = 0.424

Tables 2.16-2.18 give the details of standard deviation of ratio of the number of silanols reacted by TMMS per aminosilane bonded to the silica

Table 2.16 Absolute S.D. SiOH/Aminosilane for 200DF silica

Aminosilane	SiOH reacted/aminosilane	Standard Deviation
APTES	0.560	0.193
ABTES	0.782	0.205
AEIDMS	0.773	0.220
APDMES	1.153	0.424

Table 2.17 Absolute S.D. SiOH/Aminosilane for HP39 silica

Aminosilane	SiOH reacted/aminosilane	Standard Deviation
APTES	1.120	0.159
ABTES	1.216	0.156
AEIDMS	0.587	0.145
APDMES	1.292	0.222

Table 2.18 Absolute S.D. SiOH/Aminosilane for 200DF silica

Aminosilane	SiOH reacted/aminosilane	Standard Deviation
APTES	1.278	0.201
ABTES	1.058	0.189
AEIDMS	1.087	0.204
APDMES	1.755	0.313

The means and standard deviations in Table 2.16 were used to calculate a t-statistic, thus providing a probability value that two compared values are different. A paired t-test comparing two means with different standard deviations was applied using the following equations:

$$t = \frac{\bar{X}_1 - \bar{X}_2}{S_{X_1 X_2} \cdot \sqrt{\frac{1}{n_1} + \frac{1}{n_2}}}$$

Where

$$S_{X_1 X_2} = \sqrt{\frac{(n_1 - 1)S_{X_1}^2 + (n_2 - 1)S_{X_2}^2}{n_1 + n_2 - 2}}.$$

Where n is the number of measurements made in a group (10 in this case), S^2 is the variance

found in that group, and X (bar) is the value used for comparison of data. The number of degrees

of freedom to calculate the probability from the t-value is obtained with the following

relationship:

$$\text{d.f.} = \frac{(s_1^2/n_1 + s_2^2/n_2)^2}{(s_1^2/n_1)^2/(n_1 - 1) + (s_2^2/n_2)^2/(n_2 - 1)}.$$

2.3.2.1 Organosilanes comparisons.

In looking at trends, first comparisons of data for pairs of organosilanes will be analyzed.

1. APTES (aminopropyltriethoxysilane) and ABTES (aminobutyltriethoxysilane) were originally

chosen for comparison based on the hypothesis that the butyl group being longer than the propyl

group, can reach more silanols thus catalyzing more TMMS reactions on the surface. Table 2.19

provides the data and probabilities for the three silicas. Note that for the silica gels the hypothesis

holds that ABTES catalyzes reactions with more silanols than APTS, though the P-value for

HP39 (87%) is not very convincing. However for the fumed silica HS5 the opposite, statistically

significant trend holds. It is believed that data for HS5 must be considered separately from the

silica gels, to be discussed later.

Table 2.19 Statistics of comparison for ABTES and APTES

SiO$_2$	SiOH reacted per aminosilane APTES	SiOH reacted per aminosilane ABTES	t - statistic	Degrees of Freedom	Probability values are different (%)
200DF	0.560	0.782	4.02	13	99.7
HP39	1.120	1.216	1.99	16	87.0
HS5	1.278	1.058	4.06	15	99.8

Table 2.20 Statistics of comparison for APDMES and APTES

SiO$_2$	SiOH reacted per aminosilane APTES	SiOH reacted per aminosilane APDMES	t - statistic	Degrees of Freedom	Probability values are different (%)
200DF	0.560	1.153	4.02	13	99.7
HP39	1.120	1.292	1.99	16	87.0
HS5	1.278	1.755	4.06	15	99.8

2. Another comparison can be made between two organosilanes with the same chain length, one monofunctional (APDMES) and the other trifunctional (APTES). Data is provided in Table 2.20.All three silicas show the same trend, APDMES catalyzes more TMMS reactions with silanols than APTES. Note however that the increase with the 200DF narrow pore silica gel is highly significant (99.7%) but with the wide pore silica gel less than completely convincing (87% probability difference).

3. The third comparison is with monofunctional organosilanes APDMES and N-2-Amino ethyl 3-amino isobutyl dimethylmethoxy silane (AEIDMS) which has a longer chain with a secondary amine at the C3 position followed by a terminal primary amine at the C6 position. Probability values with corresponding data are shown in Table 2.21. Note that with both the silica gels and fumed silica there are

Table 2.21 Statistical comparison of APDMES and AEIDMS.

SiO$_2$	SiOH reacted per aminosilane AEIDMS	SiOH reacted per aminosilane APDMES	t - statistic	Degrees of Freedom	Probability values are different (%)
200DF	0.773	1.153	2.52	13	93.00%
HP39	0.587	1.292	8.41	15	99.98%
HS5	1.087	1.755	5.66	15	99.98%

fewer silanols catalyzed per AEIDMS than with APDMES. However the trends are opposite to what one might have predicted given that there are two amines capable of catalysis with AEIDMS, and the carbon chain is longer potentially making more silanols accessible. Perhaps the two amines results in restricted motion of the chain as they interact with silanols, and steric hindrance makes the secondary amine a less effective catalyst than the terminal primary amine.

2.3.2.2 Silica comparisons.

A second way to analyze this data is to look at a given organosilane and compare the data across silicas. Table 2.22 summarizes the data compared in this manner.

Table 2.22 Probability that aminosilane catalysis of TMMS reactions (SiOH reacted / aminosilane) are different. Silica in parentheses has the larger value.

Organosilane	200DF/HP39	200DF/HS5	HP39/HS5
APTES	>99.9% (HP39)	>99.9% (HS5)	86% (HS5)
ABTES	>99.9% (HP39)	98.8% (HS5)	89% (HP39)
AEIDMS	91% (HP39)	99.2% (HS5)	>99.9% (HS5)
APDMES	25% (HP39)	99.5% (HS5)	99.7% (HS5)

87

A comparison of the silica gels 200DF and HP39 indicates a large difference in the ability of the trifunctional aminosilanes to catalyze silanols, while the ability of tethered monofunctional amines show arguably statistically insignificant differences. Given the ability of trifunctional silanes to undergo cross-linking reactions, it is possible that this difference can be explained by the narrow pores of 200DF being inaccessible to TMMS after reaction with APTES and ABTES. This would not be nearly as much of an issue with the wider mesoporous HP39. If silanols within narrow pores are inaccessible to TMMS then those silanols will not be reacted, reducing the SiOH reacted/aminosilane values.

In all cases the ratio of SiOH reacted/aminosilane is greater for HP39 than 200DF. In comparing the same ratios for 200DF and the fumed silica HS5, in all cases HS5 gives a higher ratio. In fact reactions on HS5 give a statistically significant higher reaction ratio than HP39 for the monofunctional silanes. With the trifunctional silanes the differences between HS5 and HP39 are not entirely convincing. It is interesting to consider why the monofunctional silane ratio would be so much higher for HS5, given the fact that the silanol concentration per nm^2 is considered to be much less for fumed silicas compared to silica gels. Furthermore it was previously argued that the wide HP39 pores are not likely to be sufficiently narrowed to exclude TMMS which would reduce the measured ratios. Given these arguments one would expect HP39 to have a higher ratio of silanols reacted per aminosilane compared to HS5. However that HS5 is composed of solid, non-porous primary particles of approximately 10 nm (or less), and that the porosity is obtained from these primary particles interacting to form aggregates. Thus any aminosilane is reacted on the external surface of a primary particle, and given the nanometer scale can have a relatively high diffusion constant compared to a micron sized silica gel particle.

88

Thus an aminosilane on HS5, while tethered, may have the ability to catalyze many silanols on a variety of other particles. This could explain why the silanol/aminosilane ratio is so high on HS5 modified silicas.
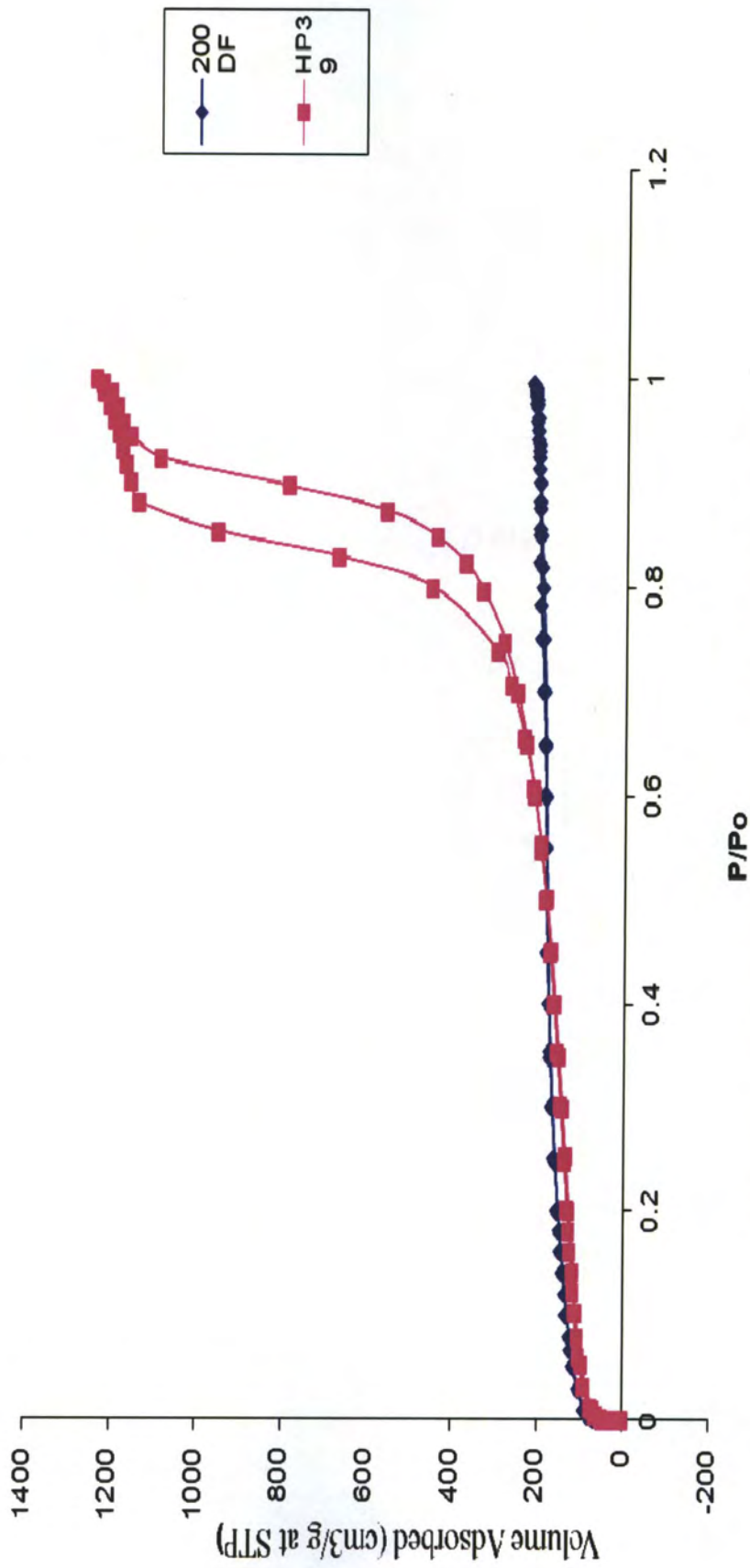
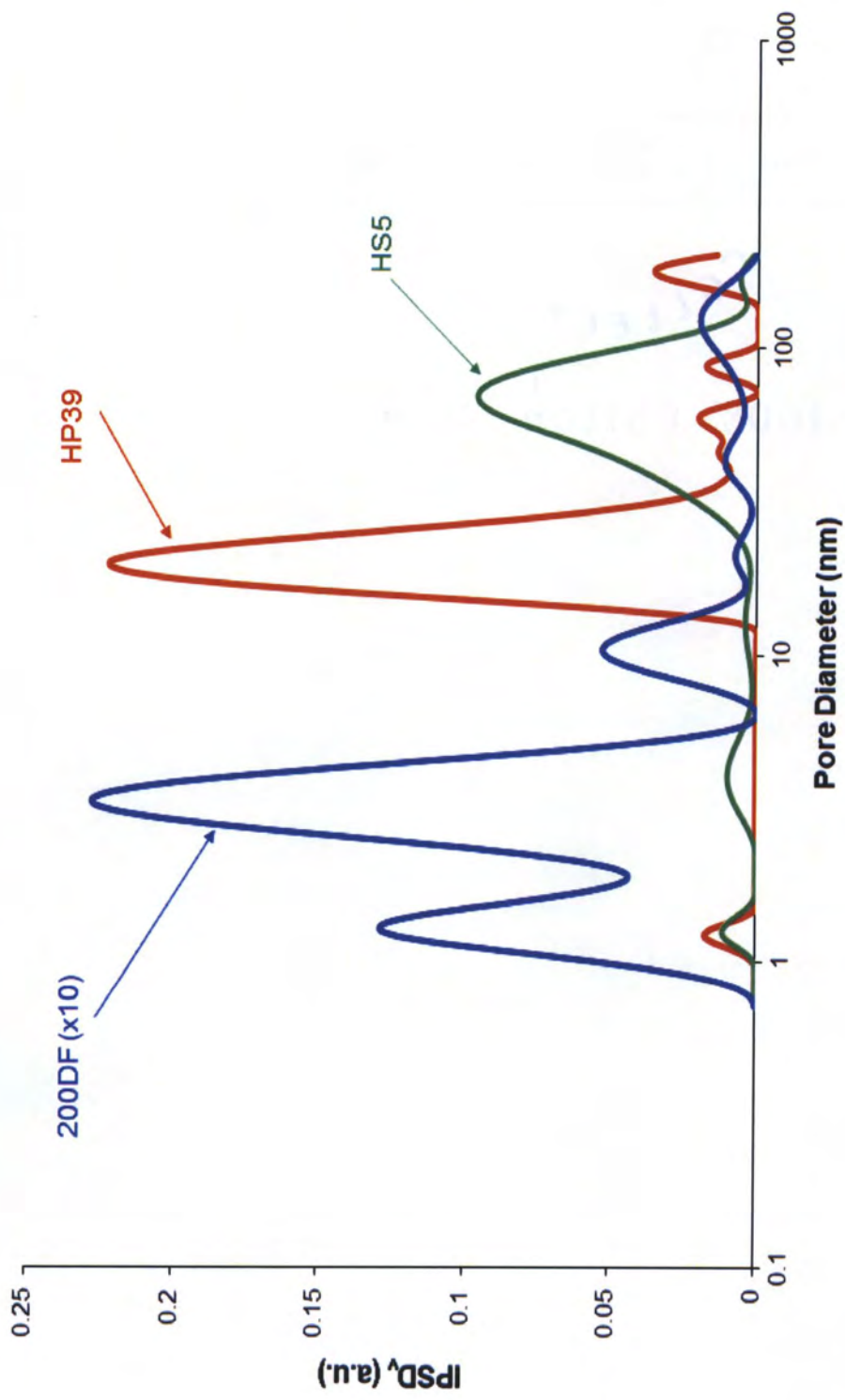Figure 2.6 Nitrogen adsorption isotherms of silica gels HP39 and 200DF

Figure 2.7 Pore size distribution compared to the pore volume for unmodified silica gels HP39, 200DF and HS-5.
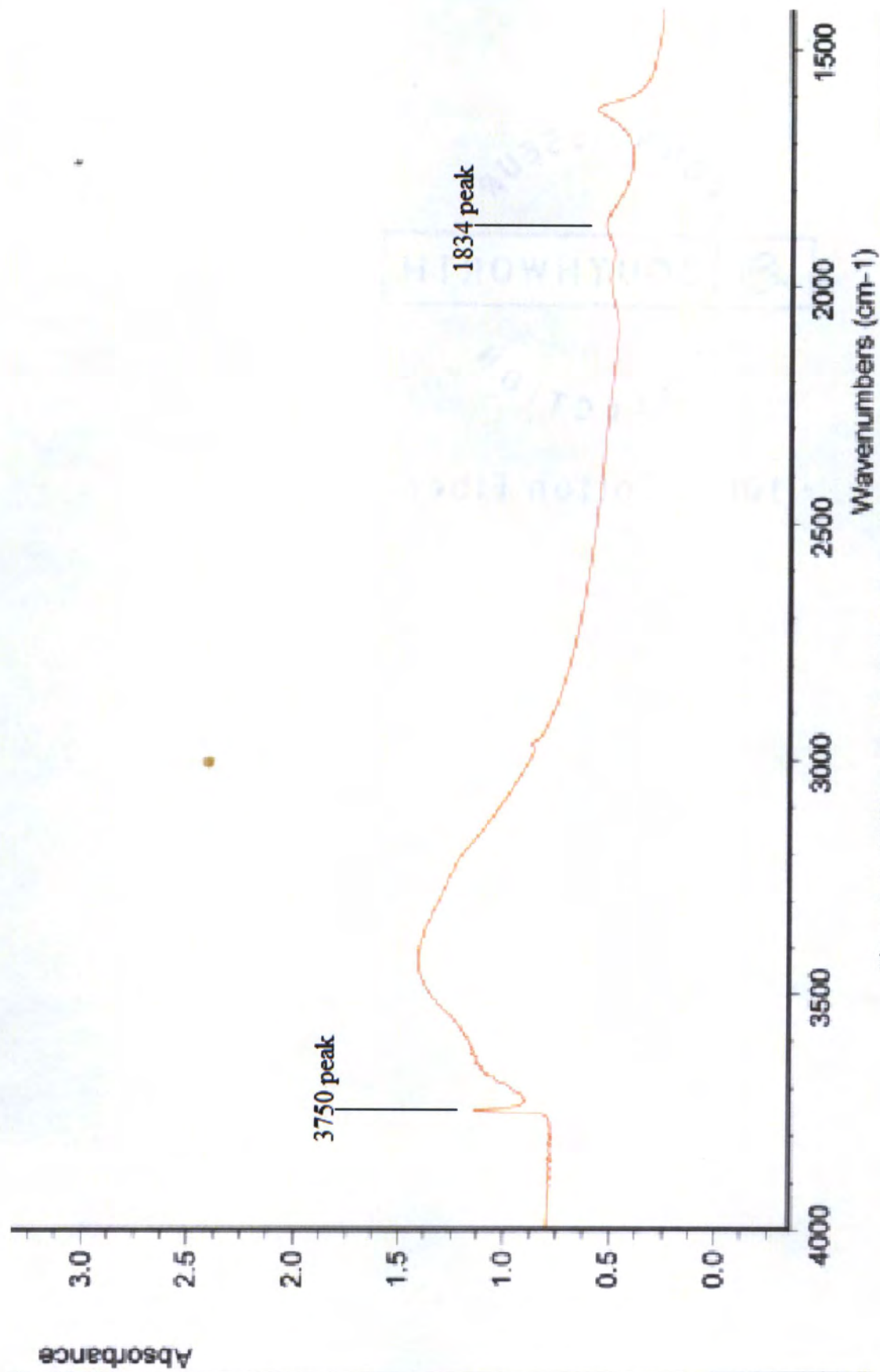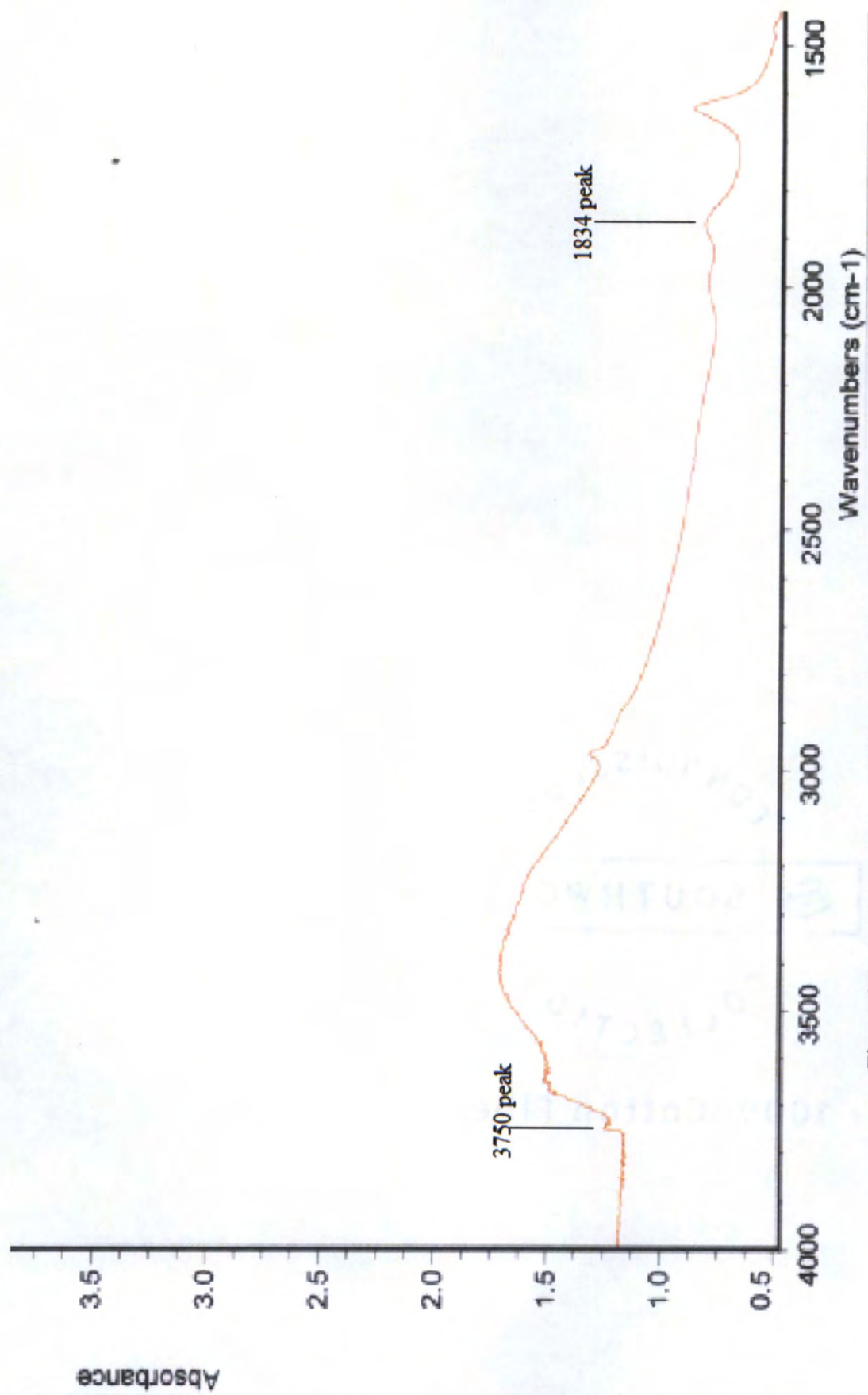
Figure 2.8 : FTIR spectrum of HS-5 silica with toluene

92

Figure 2.9 : FTIR spectrum of HS-5 silica with aminosilane AEIDMS

2.4 Conclusion

From the results the grafting behavior of aminosilane on the surface of the silica strongly depends on the number of amine groups, length of the propyl chain, number of alkoxy groups and the type of silica. Monoalkoxysilane APDMES is the one which catalyzed the highest amount of TMMS which determines that for postsynthetic modifications monoalkoxysilanes can be used instead of trialkoxysilanes for maximum results. Increase in the amine groups in a molecule may increase its chances for forming clumps or restrict their movement which was observed from the poor catalysis of TMMS by AEIDMS. Multiple bonds formed by trialkoxysilanes (APTES, ABTES) to the surface may limit the "reach" of the amine group by reducing the molecule's flexibility. Increase in the chain length of the catalyzing arm increased the catalyzation of ABTES than APTES. Oligomerization may result in a reduction in pore size especially for the narrow pore silica gel which was seen by the low catalysis of TMMS by trialkoxysilanes. Future studies include the use of different lengths of propyl chains of same aminosilane to exactly determine the way the surface hydroxyl groups are distributed on the silica.

2.5 References

1. R.K. Iler "The Chemistry of Silica" *Wiley Interscience*, 1979.

2. L.T. Zhuravlev; *Langmuir* 1987, 3, 316.

3. Gilpin, R. K., and Gangoda, M. E., *J. Chromatogr. Sci.* 1983, 21, 352

4. *Analytical and Bioanalytical Chemistry* 2006, 386, 1649.

5. U.S. Patent No. 5,900,315, Charles B. Little, Cabot Corporation, 1999.

6. E.P. Plueddemann, Silane coupling agents, 2nd ed., Plenum Press, New York, 1991, 64

7. J.P. Blitz, R.S.S. Murthy, D.E. Leyden; "Ammonia Catalyzed Silylation of Cab-O- Sil with Methoxymethylsilanes", *Journal of the American Chemical Society* 1987, 109, 7141.

8. J.P. Blitz, R.S.S. Murthy, D.E. Leyden; "The Role of Amine Structure on Catalytic Activity for Silylation Reactions with Cab-O-Sil", *Journal of Colloid & Interface Science* 1988, 126, 387.

9. Hanna Salmio and Dominik Bruhwiler, *J. Phys. Chem. C* 2007, 111, 923.

10. J.P. Blitz, R.S.S. Murthy, D.E. Leyden; "Studies of Silylation of Cab-O-Sil with Methoxymethylsilanes by Diffuse Reflectance FTIR Spectroscopy", *Journal of Colloid & Interface Science* 1988, 121, 63.

11. Changhua C. Liu and Gary E. Maciel, *J. Am. Chem. Soc.* 1996, *118,* 5103.